Fundamental Studies of Ignition Process in Large Natural Gas Engines Using Laser Spark Ignition

Final Report

Reporting Period Start Date:	May 1, 2002
Reporting Period End Date:	June 30, 2008
Principal Authors:	Dr. Azer Yalin Dr. Bryan Willson
Report Date:	April 2008
DOE Award Number:	DE-FC26-02NT41335
Submitting Organization:	Engines & Energy Conversion Laboratory Colorado State University Fort Collins, CO 80523-1374 USA

Disclaimer

This report was prepared as an account of work sponsored by an agency of the United State Government. Neither the United State Government nor any agency thereof, nor any of their employees, makes any warranty, express or implied, or assumes any legal liability or responsibility for the accuracy, completeness, or usefulness of any information, apparatus, product, or process disclosed, or represents that its use would not infringe privately owned rights. Reference herein to any specific commercial product, process, or service by trade name, trademark, manufacturer, or otherwise does not necessarily constitute or imply its endorsement, recommendation, or favoring by the United State Government or any agency thereof. The views and opinions of authors expressed herein do not necessarily state or reflect those of the United States Government or any agency thereof.

Abstract

Past research has shown that laser ignition provides a potential means to reduce emissions and improve engine efficiency of gas-fired engines to meet longer-term DOE ARES (Advanced Reciprocating Engine Systems) targets. Despite the potential advantages of laser ignition, the technology is not seeing practical or commercial use. A major impediment in this regard has been the "open-path" beam delivery used in much of the past research. This mode of delivery is not considered industrially practical owing to safety factors, as well as susceptibility to vibrations, thermal effects etc. The overall goal of our project has been to develop technologies and approaches for practical laser ignition systems. To this end, we are pursuing fiber optically coupled laser ignition system and multiplexing methods for multiple cylinder engine operation. This report summarizes our progress in this regard. A partial summary of our progress includes: development of a figure of merit to guide fiber selection, identification of hollow-core fibers as a potential means of fiber delivery, demonstration of bench-top sparking through hollow-core fibers, single-cylinder engine operation with fiber delivered laser ignition, demonstration of bench-top multiplexing, dual-cylinder engine operation via multiplexed fiber delivered laser ignition, and sparking with fiber lasers. To the best of our knowledge, each of these accomplishments was a first.

Table of Contents

Abstract 2
Table of Contents 3
List of Figures 4
List of Tables 5
Executive Summary 6
1. Introduction 8
2. Fiber Optic Delivery 9
2.1 Figure of Merit and Analysis of Fiber Delivery Challenges 9
2.2 Setup for Fiber Optic Characterization 12
2.3 Coated Hollow Fibers 13
2.3.1 Beam Quality and Sparking Tests (1-m fibers) 14
2.3.2 Practical Hollow Fiber Configurations (2-m Fibers) 17
2.4 Conventional Solid Step-Index Silica Fibers 18
2.5 Photonic Crystal Fibers 21
3. Multiplexing 23
3.1 Mechanical "Step-And-Hold" Multiplexer – Bench Tests 24
3.2 Development of Multiplexer for On-Engine Use 26
4. Single-Cylinder Testing on Waukesha VGF Engine 28
4.1 Mounting Hardware 28
4.2 Engine Controller 29
4.3 Engine Test-Results 30
5. Dual-Cylinder Testing on Caterpillar 3516C engine 32
5.1 Mounting Hardware 32
5.2 Engine Controller 34
5.3 Preliminary Engine Testing 35
6. Conclusions 36
References 38
Appendix A - Fiber Laser 40
Appendix B - Technology Transfer Activities 42

List of Figures

Figure 1: Schematic diagram of focusing of light at exit of fiber. 10
Figure 2: Experimental set-up for fiber characterization and beam profiling. 12
Figure 3: Illustrative beam profiles for fiber with core diameter of 1 mm and length of 1 m. 13
Figure 4: Schematic diagram of solid fiber, uncoated hollow fiber, and coated hollow fiber 14
Figure 5: Schematic diagram of focusing of light after exiting a fiber. 14
Figure 6: Photograph of spark formation. 16
Figure 7: Experimental values of maximum input energy and corresponding core intensity for three different fiber core diameters. 20
Figure 8: Beam Propagation Parameter (M^2) for three different fiber core diameters. 20
Figure 9 Schematic diagram of photonic crystal fiber 21
Figure 10: Experimental setup of the power delivery system using LMA fiber. 22
Figure 11: Transmission of photonic crystal fiber 22
Figure 12: Schematic of multiplexer design 23
Figure 13: Left: Commercial laser scanner. Right: Schematic of Step-And-Hold approach 25
Figure 14: He-Ne laser beam multiplexed to six locations (spots) using a galvanometer. 25
Figure 15: Nd:YAG laser multiplexed through two hollow fibers. Left: Spark after right fiber. Right: Spark after left fiber. 26
Figure 16: Schematic of multiplexer design. 27
Figure 17: Schematic diagram of optics used in optical plug. 27
Figure 18: Photos of the on-engine mounting assembly. 29
Figure 19 : A schematic of the timing control and data acquisition system 30
Figure 20: Left: Pressure curves for laser and electrical spark ignition. 31
Figure 21: Mass fraction burned as a function of crank angle. 31
Figure 22: Diagram showing the engine from the top with the cylinders numbered 33
Figure 23: The optical spark plug exploded (top) and assembled (bottom) 33
Figure 24: Engine mounting. 34
Figure 25: Images obtained from laser ignited cylinder. 35

List of Tables

Table 1: Figures of Merit for different sources 11
Table 2: Effect of launch geometry on fiber output and on ability to spark 15
Table 3: Effect of fiber bending on fiber output and on ability to spark 16
Table 4: Effect of Launch Geometry on 2m long hollow waveguides 17
Table 5: Effect of Bending Configuration for input f # ~ 55 18
Table 6: Pulse-energy limits to avoid fiber damage 19
Table 7: Overview of multiplexer design requirements for use with hollow fibers 24
Table 8: Measured transmission (%) for individual components of the multiplexer unit 28
Table 9: Burn durations, average peak pressure, and COV of peak pressure. Laser ignition on cylinder #5. 32

Executive Summary

Past research has shown that laser ignition is a potential means to reduce emissions and improve engine efficiency of gas-fired engines to meet longer-term DOE ARES (Advanced Reciprocating Engine Systems) targets. From a fundamental point of view, the benefits of laser ignition (over conventional ignition) are due to: 1) the freedom to locate the laser spark in the middle of the combustion volume away from electrodes and walls which act as heat sinks; and 2) the higher power density of laser sparks, which lead to faster early flame growth and more robust early flame kernels. Additionally, laser ignition avoids limitations of conventional spark including erosion and dielectric breakdown, both of which become increasingly problematic as engine motored pressures increase. Past laser ignition efforts have generally employed "open-path" beam delivery, which is not considered industrially practical owing to safety factors, as well as susceptibility to vibrations, thermal effects etc. The overall goal of our project has been to develop technologies and approaches for practical laser ignition systems. (The project goal is inconsistent with the title of the project; however, very early in the life of the project the goals and milestones were re-scoped by DOE and the research team.) To enable practical systems we have pursued fiber optically coupled laser ignition systems and multiplexing methods for multiple-cylinder engine operation. The approaches are selected in order to be compact, rugged, reliable and with the potential for low-cost. For multi-cylinder operation we use a single remotely located laser source routed to multiple-cylinders via multiple fiber channels. To switch the laser source between the multiple fiber channels, a multiplexer is used. Finally, to inject the light pulsed leaving each fiber into the engine cylinder, an optical plug is used. The development of these components as well as results of bench-top testing and laser ignition engine testing are described in detail in this report.

A key challenge has been to use fiber optic cables to deliver the laser pulses. The high peak-powers required to generate laser sparks pose serious challenges on the use of fiber optics. Initial fiber tests by our group (and other research groups) have shown that conventional silica fibers are largely ineffective for spark delivery for laser ignition. We have developed a theoretical Figure of Merit (FOM) analysis to examine the effectiveness of different types of fibers for delivering high peak-power laser pulses and refocusing the outputs for creating optical sparks. The analysis allows evaluation of individual fibers as well as comparison of different fiber candidates but does not consider engineering factors such as robustness, lifetime etc. One finds that a minimum FOM of 3200-6900 $GW/cm^2/rad^2$ is required for laser spark generation in atmospheric air via a fiber-optic. Based on the FOM approach, one finds that conventional silica solid core fibers have FOM of 250 $GW/cm^2/rad^2$ making them unsuitable for spark delivery. On the other hand, coated hollow core fibers (developed by Tohuku University), photonic crystal fibers (PCFs), and certain fiber lasers have sufficiently high FOM to allow laser spark delivery. Indeed, we have shown laser spark formation through the coated hollow fibers and fiber lasers, and test results for the PCFs show their potential. We have performed extensive basic characterizations of candidate fibers including measurements of exit beam quality and focused intensities as a function of launch conditions and salient optical parameters. Particular focus has been placed on the coated hollow core fibers owing to their favorable parameters. The demonstrated success of these fibers allowed the development of fiber delivered laser ignition systems for single- and multiple-cylinder engine operation.

We have developed a practical laser ignition system employing a hollow core fiber for single-cylinder engine operation. A single-cylinder of an inline 6-cylinder Waukesha VGF turbocharged natural gas engine was used to test the laser ignition system. The primary goal of these tests was to demonstrate reliable ignition with the fiber delivered system. The tests were successful in that they showed 100% reliability in the spark creation and ignition. Combustion data showed that the laser ignited cylinder had the shortest duration for 0-10% mass burn fraction, the highest average peak pressure, and one of the lowest coefficients of variation (COV) for peak pressure.

Based on the results of the single-cylinder engine testing with the laser ignition system, we have developed a practical multiplexing system for multi-cylinder operation with a single laser source. Owing to goals of simplicity and potential for low-cost, we have focused on mechanical multiplexers (as opposed to multiplexers based on acousto-optic or electro-optic modulators). Specifically, we have developed a multiplexer system based on a "step and hold" approach using a commercial laser scanner comprised of a mirror mounted on a galvo. The mirror makes discrete stops when pointed at each fiber channel and launches the beam from the single laser into the multiple fibers. The output end of each fiber is connected to an optical plug that focuses the exiting beam (through a window) into the engine cylinder where a spark is created. The multiplexer setup was initially tested on the bench-top for reliable sparking. An on-engine setup employing the multiplexer system, vibration isolation unit, and control system was developed. Using this system with coated hollow optical fibers, we have performed laser ignition testing on two cylinders of a 16-cylinder Caterpillar G3516C engine. Initial tests at 1100 rpm and idling conditions have demonstrated the proof of principle for multi-cylinder engine operation with a multiplexer. Further work is being carried out to optimize the multiplexer system and develop an integrated diagnostic unit for combustion monitoring.

In summary, we have performed research to develop practical laser ignitions system based on fiber optic delivery. We have identified and demonstrated hollow core fibers as a suitable type of fiber optic for delivery of laser sparks. We have performed engine tests to demonstrate single-cylinder laser ignition with fiber delivery. We have shown bench-top operation of a multiplexer for multi-cylinder operation. We have used the multiplexer with hollow core optical fibers to show dual-cylinder laser ignition. The research described in this report provides a basis towards practical laser ignition systems ultimately suitable for commercial use.

1. Introduction

Since the invention of the laser in 1960, there has been an interest in the use of lasers for gas breakdown. By focusing a laser beam into a small region in a volume of gas, very high electrical fields can be produced to ionize the gas. Initial demonstrations of the use of laser sparks to ignite combustible mixtures were performed in the late 1960s [1], and in recent years a relatively large number of studies have been performed[2-4]. By tightly focusing the beam from a high-power pulsed laser in a flammable mixture, a combustion-initiating spark can be created. While several modes of ignition are possible, the most widely used process for laser ignition has been non-resonant breakdown[2, 5-7]. For commonly used nanosecond pulsed lasers (pulse duration ~5–10 ns), the non-resonant breakdown sequence is initiated by initial seed electrons, which are accelerated by the electric field and create new electrons in collisions. The process is termed electron cascade and leads to avalanche growth resulting in breakdown ionization[5]. Following the initial breakdown, much of the remaining laser energy is absorbed by an electron-neutral or electron–ion (inverse bremsstrahlung) process providing a combustion initiating spark[8].

The first on-engine tests using laser ignition was reported by Dale et. al[3]. They reported test results for a single cylinder Cooperative Fuel Research (CFR) spark ignition engine using both a focused CO_2 laser beam and conventional spark ignition as ignition sources. The laser operated at 10.6 μm, in the infrared, with pulse duration of 300 ns, and was focused into the combustion chamber by a 15 cm focal length lens through a zinc selenide window mounted in the spark plug hole for optical access. With the laser spark ignition, the lean limit was extended from an air/fuel ratio of 22.5 to 27.8 (corresponding to equivalence ratio of 0.77 to 0.62). Pressure traces revealed that a more rapid cylinder pressure rise was obtained with the laser ignition system for all air/fuel ratios tested, providing greater engine power and efficiency relative to the conventional spark ignition. Subsequent laboratory investigations of laser ignition (in constant volume combustion chambers) have also shown that laser based spark ignition is an approach that is very feasible for use in internal combustion engines[5]. Briefly, the differences (potential benefits) of laser spark ignition stem from two sets of effects: The first is associated with the ability to freely locate the spark within the combustion volume (by the selection of appropriate focusing optics) and the obviation of electrodes (which act as heat sinks and may provide catalytic chemistry), while the second is related to inherent physical differences between the two types of spark, for example, the higher pressure and temperature of laser sparks can lead to elevated (overdriven) early flame speed in laser ignition[8].

At the time of the initial conception of this project, these investigations by other researchers were at the “proof of concept” stage. The research had shown potential benefits of laser ignition but had not done so in a manner that could be considered practical for commercial (field) use. A major impediment in this regard has been the “open-path” beam delivery used in much of the past research. This mode of delivery is not considered industrially practical owing to safety factors, as well as susceptibility to vibrations, thermal effects etc. This shortcoming has been considered critical by engine manufacturers associated with the Advanced Laser Ignition System (ALIS) Consortium who have identified fiber optic beam delivery (for laser spark ignition) as a practical requirement for a viable laser ignition system. Thus, a major focus of the current research has been on identifying potential fiber candidates and developing a fiber optic based system for spark

delivery that can deliver nanosecond pulses with enough ignition energies. The efforts are geared towards ignition sources for high brake mean effective pressure (bmep) natural gas engines that are typically used for power generation and gas compression.

The development of components for practical laser ignition system and results of bench-top testing and laser ignition engine testing are described in detail in this report. Section 2 of the report discussed fiber optic delivery including evaluation and characterization of candidate fibers. Section 3 of the report discusses development of a multiplexer system for multi-cylinder operation using a single laser source. Engine test results for single- and dual-cylinder engine testing are described in Sections 4 and 5. Finally, conclusions are presented in Section 6.

2. Fiber Optic Delivery

2.1 Figure of Merit and Analysis of Fiber Delivery Challenges

The key challenges associated with the use of fiber optic delivery are the intensity damage threshold of the fiber optic material and limitations on focusing fiber optically delivered light. The former point relates to material properties of fiber material and limits the maximum achievable optical intensity (power per area) at the fiber exit (e.g. 1-6 x 10^9 W/cm^2 for conventional silica fibers)[9, 10]. Because the intensity at the fiber exit is limited, the imaging requirements (to generate a sufficient intensity to spark at the desired fiber location) become more stringent. The problem is compounded by the second challenge, which is the difficulty in focusing fiber optically delivered light. If one considers multimode fibers as generally needed to carry the required energies, then light exiting the fiber is difficult to focus for three reasons: the diameter of the fiber is large compared to the wavelength of the light, the light is divergent upon exiting the fiber, and (in general) the spatial quality (described by the M^2 parameter) of light exiting the fiber is degraded relative to the input light (thus increasing diffraction effects).

Here, we provide a theoretical analysis to compare different types of fibers (as well as fiber lasers), in terms of their effectiveness for creating optical sparks. The primary result of this analysis is the derivation of a "Figure of Merit", FOM_{Source}. The Figure of Merit explicitly shows the effect of various parameters on the ease of sparking and may be used to compare the ease with which different sources (i.e. fiber types or fiber lasers) can be focused to high intensity to produce sparks. It does not include engineering factors such as robustness, lifetime etc. Light exiting a fiber is schematically illustrated in Fig. 1. The Figure of Merit is proportional to the optical intensity attainable at the spark location for fixed focusing optics. Thus, it is a means to compare the appropriateness of the light at the fiber exit for sparking, irrespective of the focusing optics.

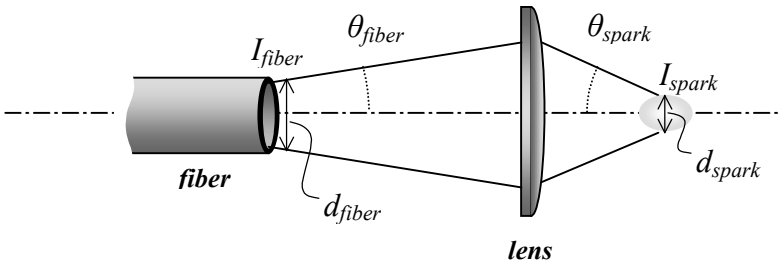

Figure 1: Schematic diagram of focusing of light at exit of fiber. Ifiber represents the optical intensity at the exit of the fiber, Ispark represents the optical intensity at the desired spark location. Similarly, dfiber and dspark represent the diameter at the fiber exit and spark location respectively. θexit and θspark represent the angles (of the widest light rays) at the fiber exit and spark location respectively

The Figure of Merit may be most simply derived with paraxial ray-tracing (geometric optics) but can be equivalently found with M^2 considerations. In order to produce a spark after the fiber, one needs to use a lens to demagnify the light at the fiber exit when imaging it at the desired spark location. By demagnifying the light, one concentrates its power into a smaller area, thereby raising its intensity (which is necessary to spark). We make the simplifying assumption that the light at the fiber exit (uniformly) fills the fiber diameter. Ray tracing allows the following expression for demagnification (Demag):

$$Demag \equiv \frac{d_{exit}}{d_{spark}} = \frac{\theta_{spark}}{\theta_{exit}} \tag{1}$$

Because we define the Figure of Merit to be independent of the focusing optics, we normalize the intensity at the spark location by the (square of the) final focusing angle at the spark location (since this angle depends on the lens used, *not* the fiber):

$$FOM_{Source} \equiv \frac{I_{spark}}{\theta_{spark}^{\ 2}} = \frac{I_{exit} Demag^2}{\theta_{spark}^{\ 2}} = \frac{I_{exit}}{\theta_{exit}^{\ 2}} \tag{2}$$

The above expression (2) for the Figure of Merit is useful for cases where the exit angles are known; however, in other cases researchers report the laser M^2 parameter as opposed to the exit angle. In such cases one can analytically show that the Figure of Merit is given as:

$$FOM_{Source} \equiv \frac{I_{spark}}{\theta_{spark}^{\ 2}} = I_{exit}\left(\frac{\pi d_{exit}}{2M^2\lambda}\right)^2 \left(= Power_{exit}\ \pi\left(\frac{1}{M^2\lambda}\right)^2\right) \tag{3}$$

We now consider the minimum FOM_{Source} required to spark (and initiate combustion). Based on past research by other groups, we assume that one requires an intensity at the spark location of approximately 2×10^{11} W/cm^2 [5, 10-13] and that (owing to aberrations) the best one can do for imaging is θ_{spark} = 0.17-0.25 radians (which corresponds to f# = 2-3) then the required figure of merit is:

$$FOM_{Source} \geq 3200 - 6900 \text{ GW/cm}^2/\text{rad}^2 \tag{4}$$

In summary, the Figure of Merit reflects the ease with which different sources (i.e. fiber types or fiber lasers) can be focused to high intensity to produce sparks. The higher its Figure of Merit, the more appropriate a given fiber is for spark delivery. The minimum required Figure of Merit to enable spark generation is approximately 3200-6900 GW/cm^2/rad^2 (from equation (4)). The Figure of Merit does not include engineering factors such as robustness, lifetime etc. Note that the Figure of Merit (equation (2)) clearly shows that in order to achieve a high intensity at the intended spark location, one requires a high intensity at the fiber exit, I_{exit}, as well as a low divergence (θ_{exit}) at the fiber exit. The requirement of a low exit angle is essentially the same as the requirement of a low M^2 parameter (see equation (3)) since a beam with low divergence corresponds to a high beam spatial quality.

As a means to compare different sources, and to gauge the effectiveness of a given source for creating sparks, we evaluate the Figure of Merit for different available solid fiber optics, hollow core fiber optics, and fiber lasers. Results (for standard nanosecond lasers) are given in Table 1 below. For cases where the exit angle is known, the Figure of Merit is evaluated using equation (2), while in cases where the M^2 parameter is known we use equation (3).

Table 1: Figures of Merit for different sources

Source	I_{exit} **(GW/cm^2)**	θ_{exit} **(Rad)**	d_{exit} **(μm)**	λ **(μm)**	M^2	FOM_{Source} **(GW/cm^2/rad^2)**
Solid Fiber (base NA)	~3	~0.11				**~250**
Hollow Fiber	~2	~0.02				**~5,000**
Photonic Crystal Fiber	~12	~0.04				**~ 7500**
Fiber Laser	~8		200	~1	6.5	**~19,000**

Solid fibers are generally characterized by their NA (Numerical Aperture) which corresponds to the exit angle (divergence angle). 1st row - Typical solid fibers operate with base NA=0.11. 2nd row – Published results for novel coated hollow fibers [14, 15]. 3rd row - Published results for photonic crystal fiber[16]. 4th row - Published results for fiber laser from reference[17].

The Figure of Merit estimates provided in Table 1 allow conclusions regarding the potential utility of different fiber types for laser ignition. Recall that a high Figure of Merit is desirable, and a Figure of Merit of at least ~3200-6900 GW/cm^2 is needed to spark. We reach the following conclusions:

1. Solid fibers operated in their standard configuration (i.e. at their base Numerical Aperture) are overly divergent (high exit angle) and have very low FOM_{Source}. Thus, they are very unlikely to allow sparking. In order to raise the Figure of Merit one must operate at lower exit angle (NA), through the use of low NA launches. These points and experimental characterization of hollow fibers are presented in Section 2.4.

2. Certain coated hollow fibers have significantly higher Figures of Merit than solid fibers and thus may allow sparking. Their high Figure of Merit is primarily due to a reduced exit angle in comparison to (standard) solid fibers. Indeed, we have had considerable success in

using hollow fibers for spark delivery and laser ignition. Bench-top characterization of the hollow fibers is presented in Section 2.3, while engine tests are described in Section 4.

3. Photonic crystal fibers have high Figure of Merit values and are promising as a spark delivery technology. As described in Section 2.5, we have performed initial testing of these fibers.

4. Fiber lasers have high Figure of Merit values and are promising as a spark delivery technology. We have worked in collaboration with an external partner (University of Michigan) to demonstrate spark-delivery with fiber lasers[18]. This approach has not yet been tested on engine and is included in this report as Appendix A.

2.2 Setup for Fiber Optic Characterization

A critical aspect of our research has been to evaluate the optical properties (launch conditions, exit beam quality, exit beam divergence etc.) of various fiber optics. These efforts allow us to evaluate fiber candidates in a rigorous way that can be related to the Figure of Merit analysis. Here, we describe the general setup employed for these characterizations. A Spiricon laser beam profiling system was used to measure beam profiles at different locations upstream and downstream of the fibers. The profiling system consists of a charge coupled device (CCD) camera, frame grabber, and software that converts the beam images to quantitative spatial intensity maps. CCD cameras are very sensitive devices - if the entire beam exiting the pulsed Nd:YAG (Neodymium-doped Yttrium Aluminum Garnet) laser was directed into the camera it would be destroyed. For this reason beam splitters and neutral density filters are used to send only a small portion of the beam into the camera. The percentage of the beam sent to the CCD camera is varied based on laser energy, but typically less than 1% of the beam is used to form an image. The profiling setup is shown in Figure 2.

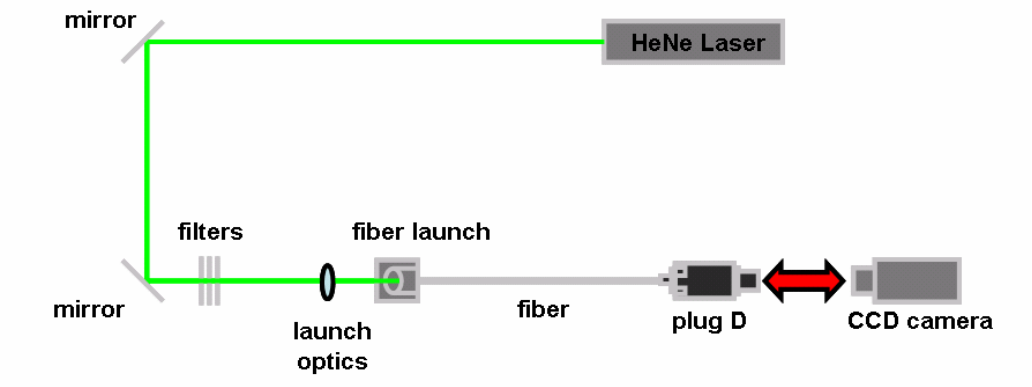

Figure 2: Experimental set-up for fiber characterization and beam profiling**.** The laser source, fiber, and Plug D can all be changed for testing with different lasers, fibers, and focusing optics.

As means of illustration we show examples of simple beam profiles obtained with a conventional silica fiber with a core diameter of 1 mm and a length of 1 m. Figure 3 shows

profiles obtained at different positions beyond the fiber exit. Simple focusing optics have been used to focus the fiber exit. In this case, the minimum (measured) spot size of the focused beam is 640 μm.

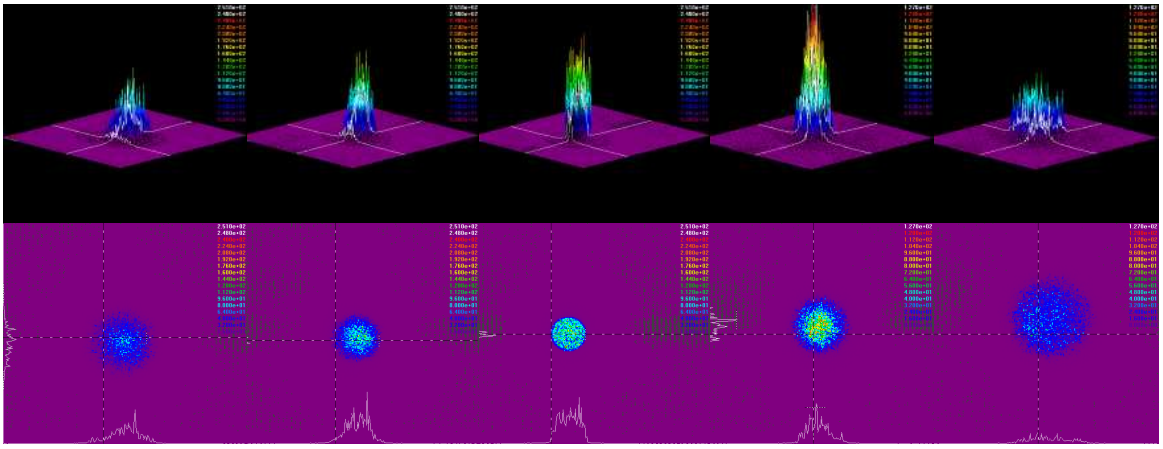

Figure 3: Illustrative beam profiles for fiber with core diameter of 1 mm and length of 1 m. For the positions shown, measured beam waist diameters (from left to right) are 860μm, 780μm, 640μm, 840μm, and 1480μm.

2.3 Coated Hollow Fibers

As shown above, coated hollow fibers have a high Figure of Merit and are potentially attractive as a means to deliver laser light to form combustion-initiating sparks. As will be described in this section and later in the report, considerable success has been achieved using the coated hollow fibers (obtained from Tohoku University). Figure 4 shows the design of the coated hollow fibers and compares them with other fibers. Conventional solid core fiber optics have one optical material in the core (center channel) and a second optical material in the cladding (surrounding material). The index-of-refraction of the core material is larger than that of the cladding material and light at the core-cladding interface is "totally internally reflected" within the fiber core. Hollow core fibers have a hollow bore (no material) surrounded by a wall material. Such a configuration has a higher index in the wall than the core and does not allow efficient light guiding. Uncoated hollow fibers may only be effectively used in straight geometries. By applying coatings to the inner wall of the hollow fiber, the efficiency of light guiding can be increased (even in bent configurations). The coated hollow fibers used in this research are based on this latter concept. To our knowledge, no researchers have previously used coated hollow fibers to deliver (nanosecond) laser pulses to form sparks.

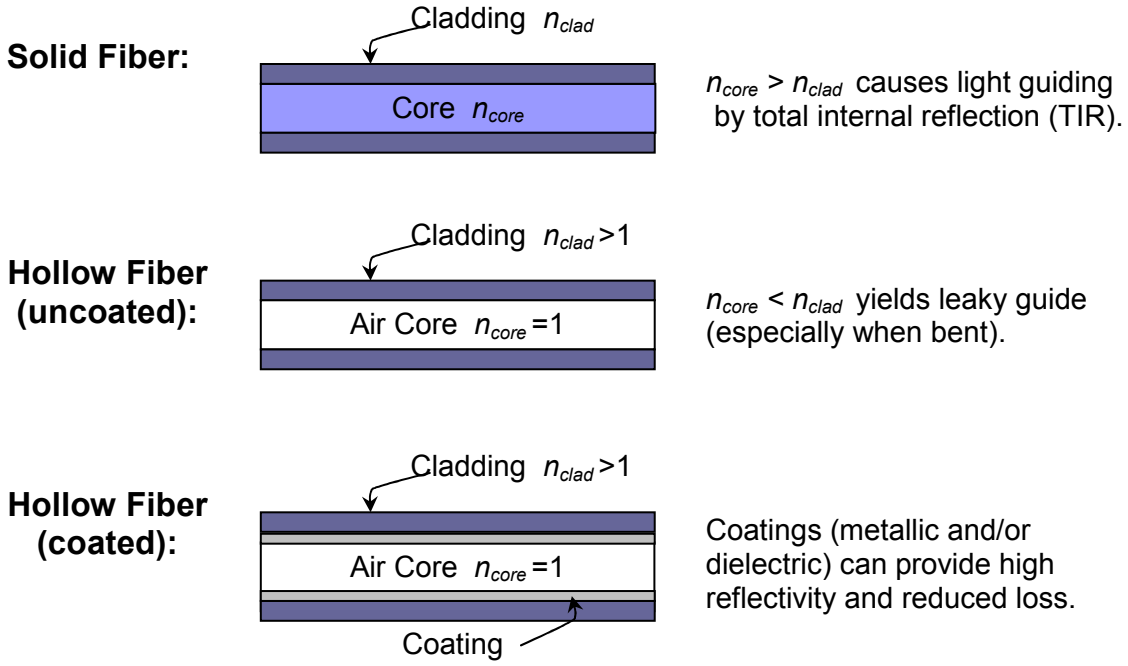

Figure 4: Schematic diagram of solid fiber, uncoated hollow fiber, and coated hollow fiber

2.3.1 Beam Quality and Sparking Tests (1-m fibers)

Figure 5 shows a cross-section of the coated hollow fiber with flexible quartz walls, the interior of which are coated with a polymer layer (cyclic olefin polymer) followed by a silver layer. The layers have precisely controlled thicknesses, and are optimized for given laser wavelengths. The manufacturing process for these fibers has been previously described [14, 19, 20]. The tests reported below use a coated fiber with an inner (hollow) diameter of 700 μm, a length of 1 m, coated for transmission at 1064 nm. For characterization, the setup is as described above and shown in Figure 2.

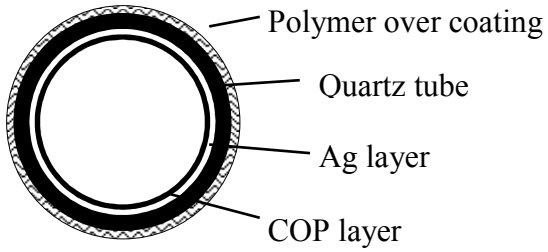

Figure 5: Schematic diagram of focusing of light after exiting a fiber.

The light source was the fundamental 1064 nm beam of a Q-switched Nd:YAG laser (Continuum 8050) with pulse duration = 7 ns, repetition rate = 5 Hz, and near diffraction-limited

spatial quality (M^2: as given by manufacturer). A single lens (left of fiber) was used to launch the laser light into the fiber while a lens pair is used to focus light exiting the fiber into a small spot where a spark may form. We have examined the effect of the launch geometry (angle) on the fiber exit parameters. We have varied the launch angle by using a series of different launch lenses: plano-convex lenses of 15, 30, and 50 cm focal length (f_{launch}). The (collimated) beam diameter incident on the launch lens was about 1 cm. The focused beam waist following each launch lens was made to be coincident with the plane of the fiber input face. To enable optimal energy transmission and exit beam quality, we followed Matsuura et al[14] and precisely aligned the initial ~10 cm of fiber length (relative to the input beam) using a 5-axis mount (3 spatial axes and 2 tilt axes). A weak helium purge was employed at the fiber input location to counter possible breakdown, and the fiber was held in a nominally straight position. For each configuration, we measured the launch input angle (θ_{launch}), beam waist (w_{launch}) at the fiber input face, the exit angle (θ_{exit}), and the energy transmission. Beam waists are taken as twice the variance of the spatial intensity profile (following M^2 conventions). Uncertainty in all reported parameters is about 10%. We also employed a pair of positive double-convex lenses located 30 cm downstream of the fiber exit to refocus the light and assess the possibility of forming sparks. The first (upstream) lens had a focal length of 35 mm, while the second lens had focal length of 9 mm and was located 30 mm behind the first. This lens pair was positioned to yield the minimum spot size (without overfilling the optics) and was experimentally found to offer high demagnification. Experimental results are given in Table 2 and discussed below.

Table 2: Effect of launch geometry on fiber output and on ability to spark

f_{launch} (cm)	θ_{launch} (rad)	w_{launch} (μm)	θ_{exit} (rad)	Spark Formation
15	0.033	47	0.031	No
30	0.017	65	0.018	Intermittent
50	0.010	77	0.009	Yes

Similar to Matsuura et al, we found transmission efficiencies (through the 1 m fiber) of about 80% at low power and a reduced transmission of ~70% at the peak transmitted energy of ~50 mJ (corresponding to an average intensity of ~1.9 GW/cm^2 at the fiber exit). We found the peak energy and transmission values to be quite insensitive to the launch lens within the range of focal lengths tested, so that these values apply to each of the three launches. The measured beam waists at the launch were consistent with those from M^2 theory. For example, for the 50 cm launch the waist of 76 μm on the fiber input face was consistent with that predicted by M^2 theory ($w \approx M^2(\lambda/\pi)(f/w_0) \approx 67$ μm), with the slight under-calculation likely due to aberration by the launch lens. For the shorter focal length launches the measured waists become higher relative to the calculated values (40 μm for 30 cm launch, and 20 μm for 15 cm launch) consistent with aberration effects become more prevalent as the launch *f*# (focal length) decreases. In each case, the waist at the launch was small compared to the 700 μm fiber inner diameter which allows effective energy coupling.

We found that reducing the fiber input angle (θ_{launch}) causes the fiber exit angle (θ_{exit}) to reduce (and the two values mirror one another within experimental uncertainty). Since the optical intensity at the fiber exit was similar for each launch, we expected that the lowest angle launch would be most amenable to spark formation. Indeed, of the configurations tested (and using the

focusing optics described above) only the 50 cm launch lens allowed reliable spark delivery. For this case, we found a beam waist (at the spark location) of approximately 30 μm and a minimum energy required to spark of 39 mJ. These parameters correspond to an average optical intensity of ~200 GW/cm^2 at the spark location, consistent with published breakdown thresholds in atmospheric pressure air (order ~10^2-10^3 GW/cm^2) [5].With the 50 cm launch lens we found that the system sparks ~97% of the time. Because the breakdown threshold for sparking decreases with pressure[11] it is very likely that such configurations would spark with 100% reliability at engine conditions (as was found in later engine tests). Figure 6 shows a photograph of the optical spark.

Figure 6: Photograph of spark formation.

To assess practical implementations, we have explored the effects of fiber bending on system performance. Tests were conducted using the 50 cm launch configuration, which generated sparks when straight. In these experiments the first 40 cm of the fiber length was held straight while the remaining 60 cm of length was bent into arcs of different radii (R). Measurements of exit divergence angle (normalized by the divergence angle for the straight fiber case), fiber transmission (at peak transmitted energy), and percentage of laser shots resulting in sparks are given in Table 3. Straight fiber results are also included ($1/R$ = curvature = 0). Similar to Matsuura et al, we found that as the curvature increases, the fiber exit angle increases and transmission decreases. Both trends lead to a reduction in optical intensity at the desired spark location, and a lower percentage of laser shots creating optical sparks. The intermittent sparking at bent conditions was attributed to varying intensity profiles of the multi-mode (exit) beams.

Table 3: Effect of fiber bending on fiber output and on ability to spark

$1/R$ (m^{-1})	$\theta_{exit\ bent} / \theta_{exit\ straight}$	Transmission %	Spark Formation %
0	1.00	73	97
0.73	1.19	66	85
1.01	1.21	64	50
1.29	1.29	62	<1

These test results confirmed our ability to deliver optical sparks using the compact industrial laser and the hollow fibers, enabling us to use them in an on-engine system, the design of which is described laser in this report.

2.3.2 Practical Hollow Fiber Configurations (2-m Fibers)

In order to increase the practicality of the coated hollow fibers it is desirable to increase their length while maintaining the capability of sparking with some degree of bending. Here, we summarize tests of 2-m length coated hollow fibers. Test conditions are similar to those used for the 1-m testing (Section 2.3.1). Table 4 summarizes the effect of launch condition on the performance of the fiber. The focal length of the launch lens and input f-number are represented by f_{launch} and $f_{\#}$ respectively, while the angular beam divergence at the fiber exit is given by $\Theta_{exit.}$. The (measured) focal spot size at the waist and final focused (spark) location are represented by w_{launch} and w_{focus}. The intensities at the fiber exit and final focused (spark) location are represented by I_{exit} and I_{focus} (where the former is computed based on the fiber area and the latter based on w_{focus}). We also report the M^2 exit of the beam, fiber transmission, and the percentage of delivered sparks resulting in spark delivery.

Table 4: Effect of Launch Geometry on 2m long hollow waveguides

f_{launch} (mm)	$f\#_{input}$	w_{launch} (μm)	Θ_{exit} (rad)	M^2_{exit}	I_{exit} (GW/cm^2)	w_{focus} (μm)	I_{focus} (GW/cm^2)	Transmission %	Sparking %
135	35	27	0.014	21	0.58	35	120	80	<10
215	55	39	0.01	15	0.6	17	470	86	98
335	85	138	0.015	22	0.52	44	68	80	0

Of the conditions tested, we find optimal spark formation (~98% of laser shots) and exit beam parameters for input f# ~55. The differing optical transmissions of Table 2 as compared to that found for straight 2-m fiber in our earlier tests are due to the fact that the current tests are conducted with a different laser source (BigSky versus NewWave) and serve to demonstrate the high sensitivity of the fiber transmission to the detailed spatial mode of the launch beam. The f#~55 launch configuration resulted in the lowest beam exit divergence (Θ_{exit} ~ 0.014) corresponding to M^2 of ~15 at the fiber exit. With pulse energy of ~35 mJ for this condition, the focal intensity was as high as ~ 470 GW/cm^2 well above the break down threshold intensity[5, 13, 21, 22],. The occasional (2%) misfires are thought to be due to varying multimode spatial profile (hot spots) in the exit beam[14, 15]. We found that as the f# was increased (f# ~85) or decreased (f# ~35) in relation to this condition, the fiber transmission and the exit beam quality degraded suggesting an optimum launch f#. This behavior is consistent with past findings for hollow fibers [23] and is associated with the mode coupling and mode distribution of light in the fiber.

We have also explored the effects of fiber bending on the fiber performance. Tests were conducted for the input f# of 55, which provided the highest sparking at straight configuration. In these experiments, the first 100 cm of the fiber was kept straight while the remaining 100 cm was bent into arcs of different radii of curvature (R). As shown in Table 5 and consistent with past research[24, 25] we found that as the fiber was bent, transmission of the fiber dropped and the exit beam divergence and corresponding M^2 increased. We found that for small bending (R=1.5 m) the performance remained comparable to that of straight configuration and provided enough spatial beam quality at fiber output to give a high sparking rate (~ 98%). With further bending

(i.e. R= 1m), the sparking reduced to zero due to increase in the exit beam divergence (~ 0.019) and corresponding increase in M^2. While moderate fiber bending is possible, we identify bending-loss (transmission and beam-quality) as a limitation of hollow fibers. As will be discussed later in this report (Section 4), on-engine designs must factor in bending-loss as a constraint. Owing to the decrease in the spark formation intensity requirement (i.e. breakdown threshold) with increasing pressure, the f#~55 configuration with 1/R<~0.66 m^{-1} should spark reliably (i.e. 100%) at engine motored pressures (~200 psi+ in typical ARES class natural gas engines giving a decrease in intensity requirement of >3 assuming the $P^{-0.5}$ scaling[11]).

Table 5: Effect of Bending Configuration for input f # ~ 55

1/R	w_{launch}	Θ_{exit}	M^2_{exit}	I_{exit}	w_{focus}	I_{focus}	Transmission %	Sparking %
(m^{-1})	(μm)	(rad)		(GW/cm^2)	(μm)	(GW/cm^2)		
0	39	0.01	15	0.6	17	520	86	98
0.66	39	0.011	16	0.58	21	300	83	98
1	39	0.019	29	0.5	49	53	80	0

The performance achieved with the 2-m fiber is very adequate for the design of practical fiber delivery configurations that can be used to ignite multiple cylinders. As shown in our multiplexing work and engine testing (Section 3 and Section 4 respectively) the coated hollow fibers are also very compatible with multiplexing and multi-cylinder engine operation.

2.4 Conventional Solid Step-Index Silica Fibers

The Figure of Merit analysis shows that solid core silica fibers operated at standard conditions (numerical aperture) are unsuitable to form optical sparks at atmospheric pressure. However, spark formation becomes increasingly easier at higher pressures, as are found in the targeted engine cylinders. The reason for the increased ease of sparking is that the threshold breakdown intensity decreases with increasing pressure (I_{thr} α p^{-n}, where, n depends on the gas and lies between 0.3 and 0.9)[26]. Based on these ideas, this section discusses use and characterization of conventional fibers for high-pressure spark ignition.

Table 6 shows the typical safe energy limit for multi-mode step-index silica fibers of three different core sizes, d=400, 600 and 910 μm (values provided by the vendor). Reliable ignition of lean mixtures generally requires at least 15 mJ in the combustion region[6], so to conservatively account for fiber transmission and other optical losses (e.g. from the optical spark plug), we assume that at least 25 mJ of light must be launched into the fiber. Based on this criterion, Table 6 shows the possibility of using 600 μm and 910 μm core solid core fibers for laser spark delivery.

Table 6: Pulse-energy limits to avoid fiber damage

Core Diameter (μm)	Safe Input Energy Limit (mJ)
400	19
600	27
910	40

The experimental arrangement for measuring the output beam properties is similar to that shown in Figure 2. In this case we use a 1064 nm Nd:YAG New Wave laser with 10 ns pulses and $M^2 < 2$ as the light source. The diameter of the Nd:YAG laser beam increases with increasing power. Therefore, in order to maintain constant beam diameter, the laser was operated at 50 mJ and 10 Hz. A variable beam attenuator is used to adjust the beam power. The output of the silica fiber is very dependent on the launch condition and the alignment. In order to align the fiber, the fiber is held straight and the end of the fiber is imaged at a CCD to monitor the beam quality. A 5-axis fiber holder was used for optimizing the launch alignment. The fiber is bent to the desired radius of curvature of 50 cm in order to be close to practical situation. The output of the beam is focused with two lenses. The first lens has variable focal length (f1) so that it can collimate the light exiting the fiber, while the second one has a focal length (f2) of 9 mm (with clear aperture of 8 mm) and focuses the beam.

A series of experiments were conducted to assess the maximum achievable energies. After initial alignment, the beam power was slowly increased until the fiber failed. Results of these tests are shown in Fig. 7. The fibers with core diameters of 400 and 600 μm failed at input energy of 12 mJ and 35 mJ respectively, with input average core intensity of 0.96 GW/cm^2 and 1.24 GW/cm^2 respectively. The fiber with 910 μm core failed at input energy of 67mJ with average core intensity of 1 GW/cm^2. These energies correspond closely with the safe energy limits given above. In most cases, the fiber failed a short distance after the input end after which the transmission went to practically zero. This has been observed by other researchers for high power pulsed delivery and is attributed to various reasons such as slight misalignment, hot spots in the beam that create initial damage along the core/cladding interface etc[27, 28]. However, in some other cases, the fiber also failed at the output near the core/cladding interface (most probably due to the failure of epoxy used in SMA termination).

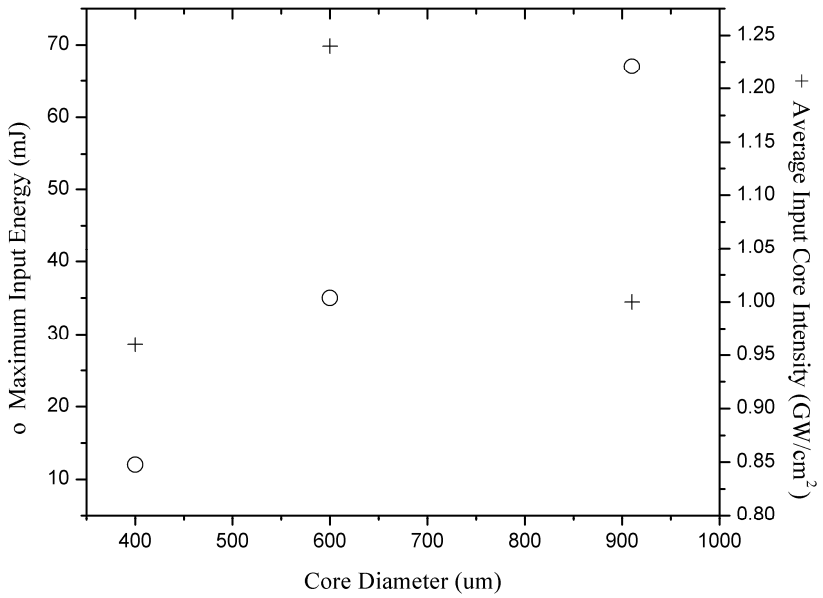

Figure 7: Experimental values of maximum input energy and corresponding core intensity for three different fiber core diameters.

Figure 8 shows the beam propagation parameter (M^2) for the same three fibers. The triangular symbols were measured for bend radii of 0.5 m(our work), while the circular symbols were measured for bend radii of 1 m[29].

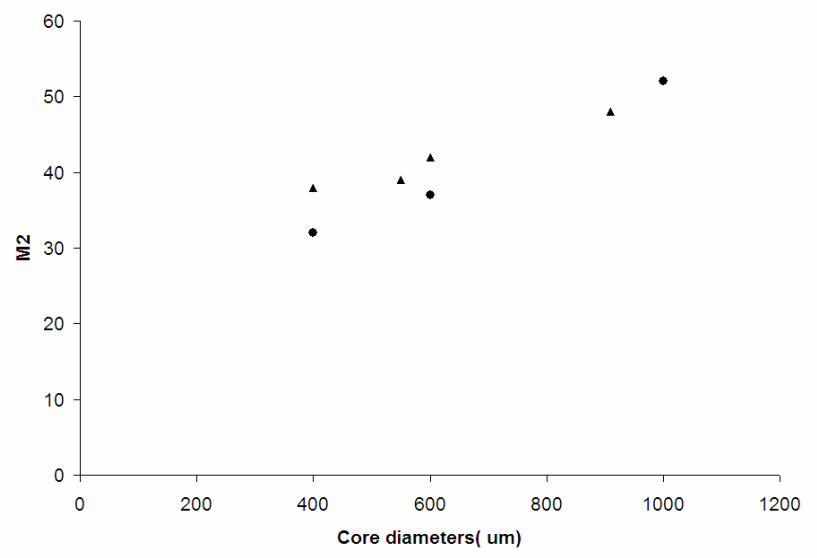

Figure 8: Beam Propagation Parameter (M^2) for three different fiber core diameters.

From the point of the safe energy limit, the 400 μm core diameter fiber is unsuitable since it cannot deliver the required pulse energy of 25mJ. The higher core diameter fibers are capable of delivering required energy, but they have beam output with relatively high M^2 (low beam-quality) making it difficult to refocus these beams to the small focal spot size required for spark formation. We have examined the possibility of spark formation by focusing the fiber outputs (through a sapphire window) into a high pressure test cell at 220 psi (characteristic of in-cylinder pressure during sparking). We were able to form laser sparks with the output of the 600 μm solid core fiber; however, the spark was not very consistent and the fiber was intermittently damaged by the high energy pulses. From our experience, it is also difficult to work with these fibers because even slight misalignment leads to higher beam quality degradation and fiber damage. In summary, we find that it is rather difficult to form sparks with the solid core fibers. Nonetheless, the results show that sparking is possible at higher pressures with conventional large core silica step-index fibers. Similar results have also been shown by G. Gaborel et al. in their work with 940 um core fiber at 6 bars with input pulse energies of 52 mJ [9].

2.5 Photonic Crystal Fibers

The photonic crystal fiber (PCF) has high Figure of Merit and is interest for beam-delivery for laser ignition. Figure 9 shows a schematic of a typical PCF. In comparison to the flexible hollow fibers, the PCFs are more tolerant of bending losses. These fibers work on the principle of modified total internal reflection. The solid silica core is surrounded by an array of hollow air cores which modifies the refractive index of the medium surrounding the core enabling single mode propagation regardless of optical wavelength.

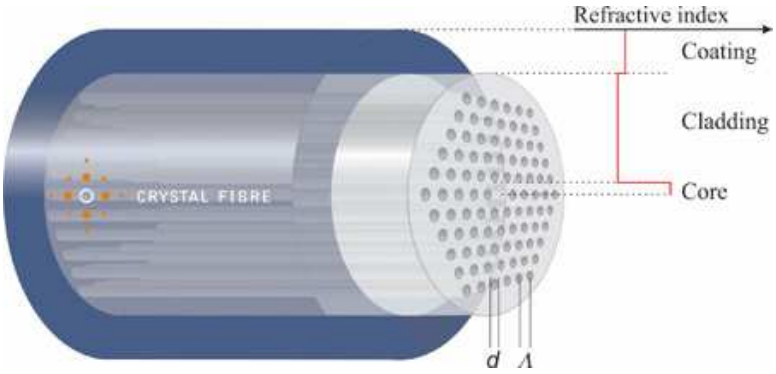

Figure 9 Schematic diagram of photonic crystal fiber

We have performed tests of solid core PCFs (LMA-25) from Crystal Fibre A/S. The tests were primarily aimed at finding the maximum energy that can be delivered through the PCFs prior to fiber damage. Figure 10 shows the experimental setup. The ends of the fiber were connectorized with high power SMA connectors. A spatial filter setup was used to improve the beam quality of the laser (M^2 ~ 1.4). A variable attenuator allows controlled attenuation of the beam from a few milli-Joules down to micro-Joules of energy without displacing the beam. The beam was

launched with a 50 mm focal length lens onto the fiber input which was held with a 5 axis fiber holder.

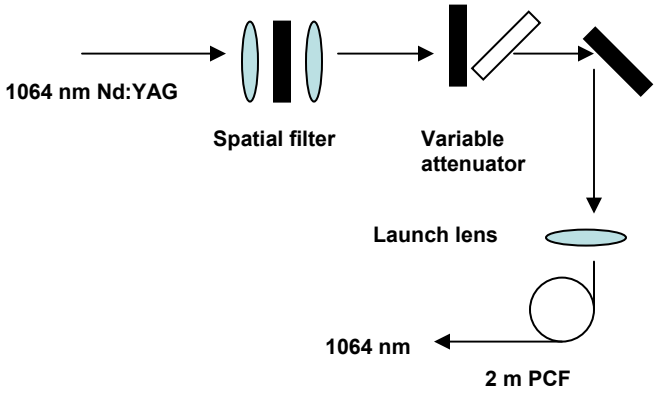

Figure 10: Experimental setup of the power delivery system using LMA fiber.

Fig. 11 shows the fiber transmission measured as a function of the input pulse energy. We found that as the pulse energy increased, the fiber transmission decreased. In these tests, the maximum achievable input energy was 1.3 mJ corresponding to an output of 0.55 mJ. While this energy level is too low for ignition of lean mixtures, it should be sufficient for certain stoichiometric mixtures.

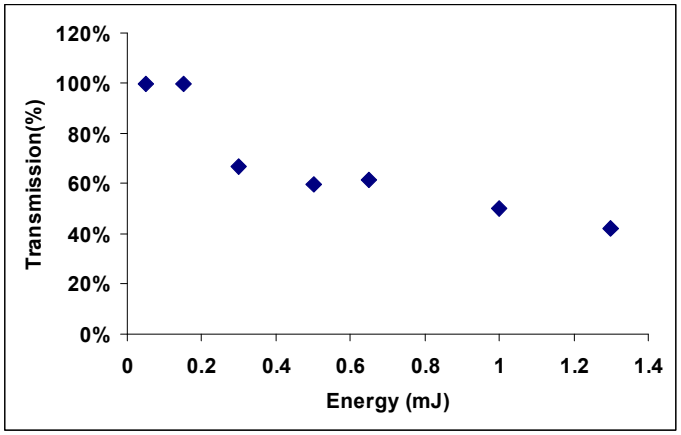

Figure 11: Transmission of photonic crystal fiber

In summary, we view that PCFs have potential for laser ignition applications owing to their high beam quality and good bending performance. The primary challenge is to delivery sufficient energy through the fibers for ignition of lean mixtures. While we view these fibers as a promising future technology, they are not considered in the remainder of this report.

3. Multiplexing

A potential advantage of the fiber delivery approach is the ability to use a single laser source multiplexed (via multiple fibers) to a series of engine cylinders (i.e. ignition areas). An example of such an approach is shown schematically in Figure 12. We have evaluated three broad approaches for the required optical switching (multiplexing). The first approach is based on the use of electro-optic modulators (EOMs) and polarizing beam splitters. A second approach is based on the use of acousto-optic modulators (AOMs) as optical switches. The AOMs rely on diffraction effects created by acoustics waves to deflect optical beams and act as switches. The final approach is based on the use of a mechanically-based system with moving mirrors acting as optical switches. In terms of selecting a multiplexing approach, we have considered factors including the expected performance, reliability, and cost. Based on these considerations we have elected to pursue mechanical switching. This selection was made due to the potential low-cost, simplicity, and high-performance of such a mechanical system. In contrast, the EOM system is high-cost and in some cases will suffer from optical losses (due to the large number of optical surfaces needed), and the AOM system is expected to have performance limitations (due to the spatial accuracy of the beam switching).

While the multiplexing designs can (with some modification) be used with different fiber delivery systems, the focus in on multiplexers for hollow core fibers, based on our successes with spark delivery through these fibers. Table 7 provides an overview of the design requirements. The required switching times and spatial accuracies are based upon parameters of the hollow fibers as well as engine-firing timings of typical ARES class engines.

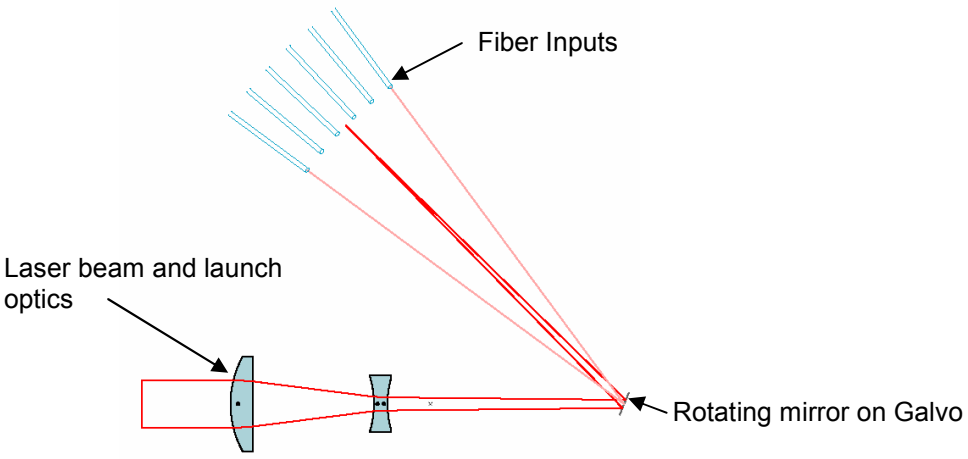

Figure 12: Schematic of multiplexer design

Table 7: Overview of multiplexer design requirements for use with hollow fibers

Mirror to Fiber length	50 mm
Fiber Spacing	5 mm
Fiber I.D	1 mm
Launch Accuracy (at fiber)	50 μm
Firing timing interval	10 ms

3.1 Mechanical "Step-And-Hold" Multiplexer – Bench Tests

We have considered two overall approaches for a mechanical multiplexer. The first is to use a mirror mounted on a continuously rotating shaft as the switching element. While this approach may be of future interest, it is not the approach we have pursued here. The approach we have developed uses a commercial "scanner" comprised of a laser on a galvanometer. The scanner is shown in the left of Figure 13. The mirror makes discrete (discontinuous) movements and we term the approach "Step-And-Hold". A schematic of the approach is shown in the right of Figure 13. We have elected to pursue this approach as the scanner is commercially available, and we view that (despite its simplicity) it will be very adequate for many implementations. (In the future, the system can be switched to a continuous rotation mode, while maintaining much of the ancillary hardware, if desired.)

To initially demonstrate the capability of the galvanometer system, we multiplexed a continuous-wave He-Ne laser into 6 locations (which simulate the inputs to 6 fibers) on a piece of paper at an equivalent engine speed of 1800 rpm (Figure 14). The test demonstrated successful performance of the galvanometer at the required speeds. The 6 bright spots on the paper correspond to the galvanometer "stopping" at the 6 required locations. If a pulsed laser was fired at these corresponding times it could be launched into the fibers. Because this test employs a continuous-wave laser, one can see a faint line between the bright spots, corresponding to the beam location as the galvanometer moves between the stop locations. In conjunction with the accuracy test mentioned above, this high-speed test shows the galvanometer should meet our specifications.

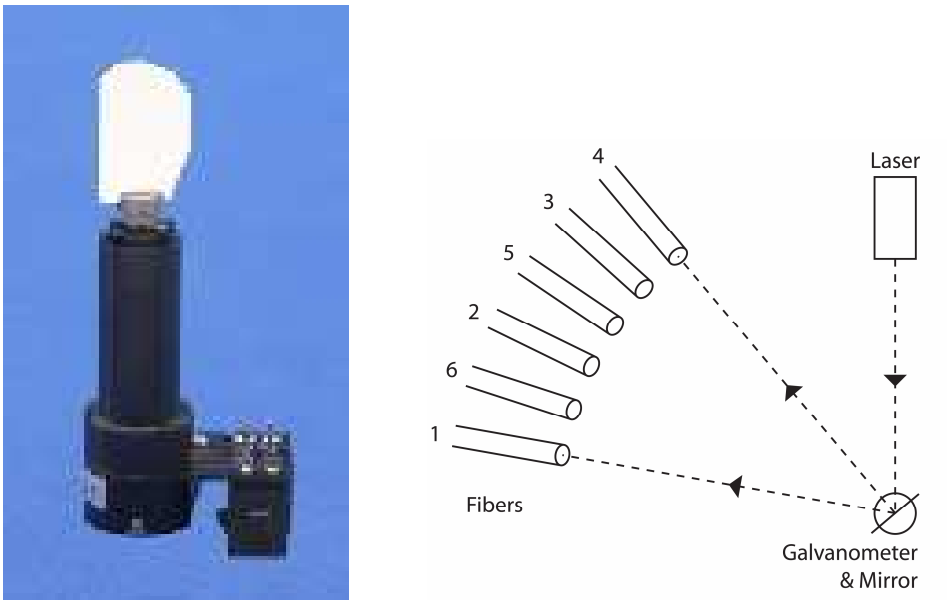

Figure 13: Left: Commercial laser scanner. Right: Schematic of Step-And-Hold approach

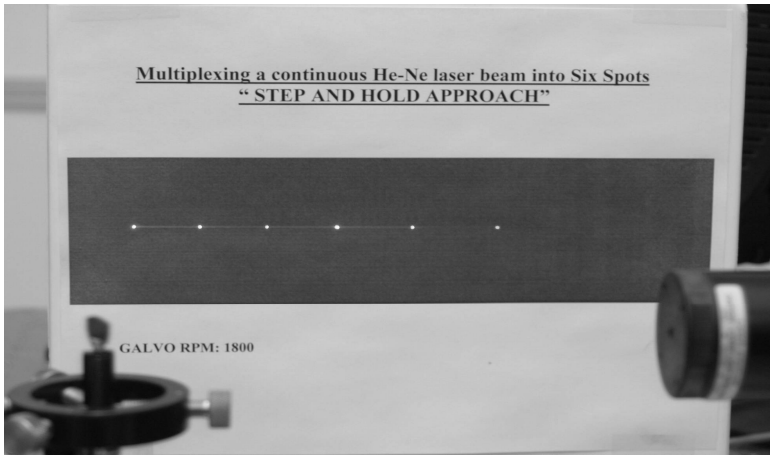

Figure 14: He-Ne laser beam multiplexed to six locations (spots) using a galvanometer.

We have also performed proof of concept testing using a pulsed Nd:YAG laser source and two hollow fibers. The setup is shown in Figure 15. In these tests we switched the multiplexer between two positions, corresponding to pointing at the two fiber entrances. We used a single focusing lens upstream of the mirror to launch the beams into the hollow fibers. In these tests, we successfully switched the laser beam back-and-forth between the two fibers. After each fiber, a laser spark was reliably produced, and the test demonstrated that the accuracy of the galvanometer was sufficient to effectively launch into the hollow fibers. Initial design calculations indicate that the galvanometer should be robust against thermal drift. According to manufacturer's specifications, for our step-sizes, the thermal angular drift per step should be less than 5 μrad/°C. Thus, for our current six step design we can tolerate a temperature drift of ~±30 °C. These tests provide the first demonstration (using any multiplexer concept) of multiplexing a pulsed laser

beam into multiple hollow fibers in a way that allows spark formation downstream of the fibers. As such, it suggests a path towards multiplexed fiber delivered laser ignition, and thus represents a significant milestone in our research.

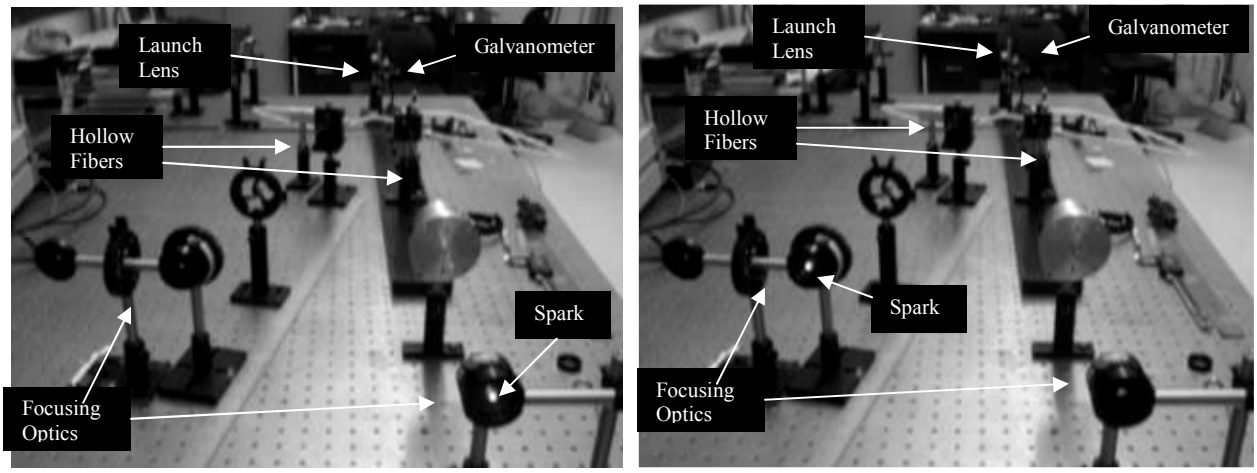

Figure 15: Nd:YAG laser multiplexed through two hollow fibers. Left: Spark after right fiber. Right: Spark after left fiber.

3.2 Development of Multiplexer for On-Engine Use

Figure 16 shows a schematic of the step-and-hold multiplexer that we've developed for engine use. Engine test results are described in Section 5. In this section we discuss the basic design as well as measurements to confirm spark delivery and examine optical loss. The current design is targeted at dual-cylinder (dual-channel) operation using the scanner as a switch, but similar designs could be used for a larger number of cylinders. (Alternatively, the scanner could be replaced with the continuously rotating shaft.) On each cylinder, an optical plug is used to receive the light from the fiber and direct it into the cylinder. Focusing optics are used to focus the light to produce the spark and a sapphire window is used for access to the cylinder. Of course, for the dual-channel system, two such optical plugs are used. The beam path in the multiplexer and optical plug is shown in the figure.

In order to characterize the multiplexer system, characterization of energy transmission (throughput), beam quality, and reliability of sparking was conducted. Figure 17 shows various locations in the setup where energy measurements were conducted. To test for energy transmission (loss) through individual component, the central section of the multiplexer was removed, and the energy was measured with a power meter at a series of locations (indicated with numbers in Fig. 17). Measuring the energy before and after a given component allows direct determination of the component's transmission. Table 8 shows the energy losses for the two channels including the individual fibers, turning mirror, collimating lens and focusing optics. The losses for the fibers are between 10% and 20% which is consistent with earlier findings. The losses through the optics are also consistent when losses are assumed to be ~4% at each surface for uncoated lens and window and ~2% at each surface for antireflection coated collimating lens. The total transmission is found as the product of that through each component (and is consistent

with an overall in/out measurement), and the total percentage loss is found as 100% minus the transmission. Total energy losses for channel 1 and channel 2 were ~32% and ~34% respectively (consistent with design expectations).

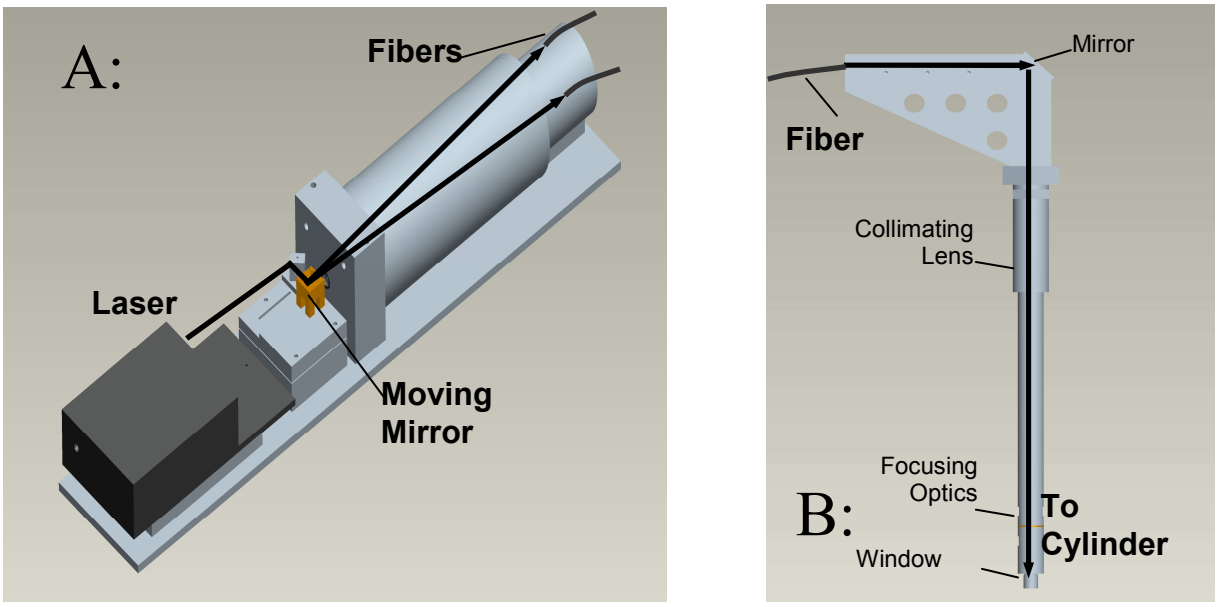

Figure 16: Schematic of multiplexer design. Black arrows show beam path. A: Laser source and multiplexer. The beam comes from the laser on the left (dark gray), is turned by a fixed mirror, then encounters the galvanometer (orange), which directs the beam to one of two fiber faces. B: Optical plug

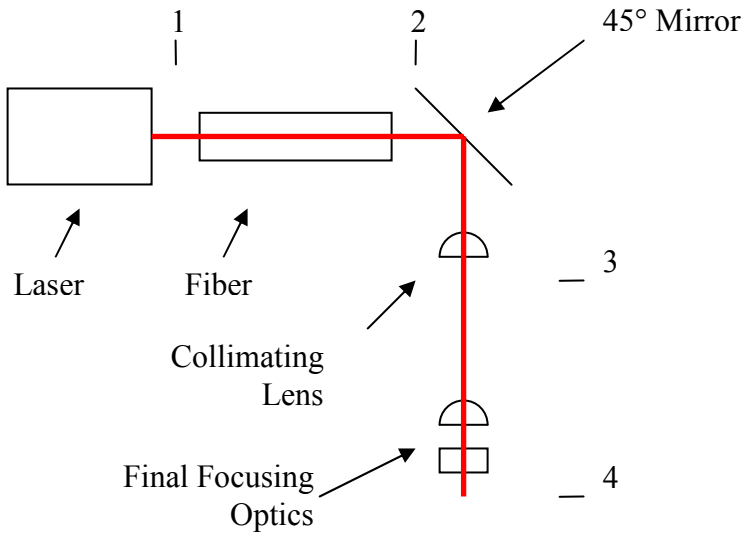

Figure 17: Schematic diagram of optics used in optical plug. Numbers indicated positions used for measurements of energy transmission and loss.

Table 8: Measured transmission (%) for individual components of the multiplexer unit

	Fiber	45 degree Mirror and Collimating Lens	Focusing Optics	Total Transmission	Total Loss
Channel 1	**83**	**96**	**85**	**68**	**32**
Channel 2	**87**	**96**	**79**	**66**	**34**

The ability to spark was investigated by setting up the multiplexer on the bench with the two fibers enclosed by nylon tubing and going straight into the optical spark plugs. A rough vacuum was drawn through the entire system in order to reduce the chance of sparking on the optical fiber faces. The laser had pulse duration of 10 ns. A high-pressure test chamber pressurized to 220 psi was used to investigate the sparking. (The pressure of 220 psi was selected to match the in-cylinder pressure of the Caterpillar G3516C engine for full throttle engine operation.) **By direct observation, it was found that 100% sparking could be obtained at the desired focal spot when the intensity was around 100 GW/cm^2, corresponding to the focused pulses with average energy of around 27mJ. This result is taken as the primary validation of desired bench-top operation of the multiplexer.**

4. Single-Cylinder Testing on Waukesha VGF Engine

In this section we discuss results of single-cylinder tests of the Waukesha VGF engine. The tests use hollow core optical fibers to deliver the laser beam, but do not use the multiplexer system (since they are single-cylinder tests). The tests serve to examine the reliability of the fiber delivery, window cleanliness, timing-control of the laser, and other practical issues.

4.1 Mounting Hardware

Having successfully demonstrated spark formation with a hollow core fiber, we have begun preliminary development of an on-engine fixture. Essentially, the laser source is coupled to the hollow fiber, which is used to deliver light to the engine cylinder. The engine mounting assembly secures all the components of the ignition system in a manner that allows for precise positioning of the laser relative to the fiber launch, and allows us to test multiple fiber bend radii. A photograph of the laser ignition system mounted to the engine is shown in Figure 18a. Guide wires help stabilize the mounting assembly from excessive vibration. Heat shields are applied to the laser, exhaust, and turbocharger to direct radiation away from the laser. The fiber and optical spark plug are not shielded, as they both are capable of withstanding temperatures in excess of 500° C.

The housing design for the fiber and associated optics is based on providing a vacuum environment for the fiber to prevent inadvertent sparking on the fiber input face. (Vacuum is achieved by connecting a compact vacuum pump to a sealed fiber system). Additionally, the housing for the fiber must withstand the high levels of heat and vibration associated with typical engine environments. For launching the beam into the fiber, and gathering the light exiting the fiber, the needed optics were held in a pair of lens tubes. The first holds the launch lens in the appropriate position and employs a pair of dowel pins to keep the tube and fiber chuck in

alignment. The second (exit) lens tube comprises a second vacuum fiber chuck that aligns the fiber with the final focusing optics. The optical spark plug contains a pair of focusing lenses which de-magnify the beam to the required intensity. Preliminary engine tests showed that we could get ignition from the laser spark created from the fiber delivery; however, it was observed that the ignition was inconsistent. This was attributed to the engine vibration that caused the frequent misalignment of the laser into the fiber and thus resulting in misfires. This problem was overcome by incorporating a vibration isolation unit as shown in Figure 18b and 18c.

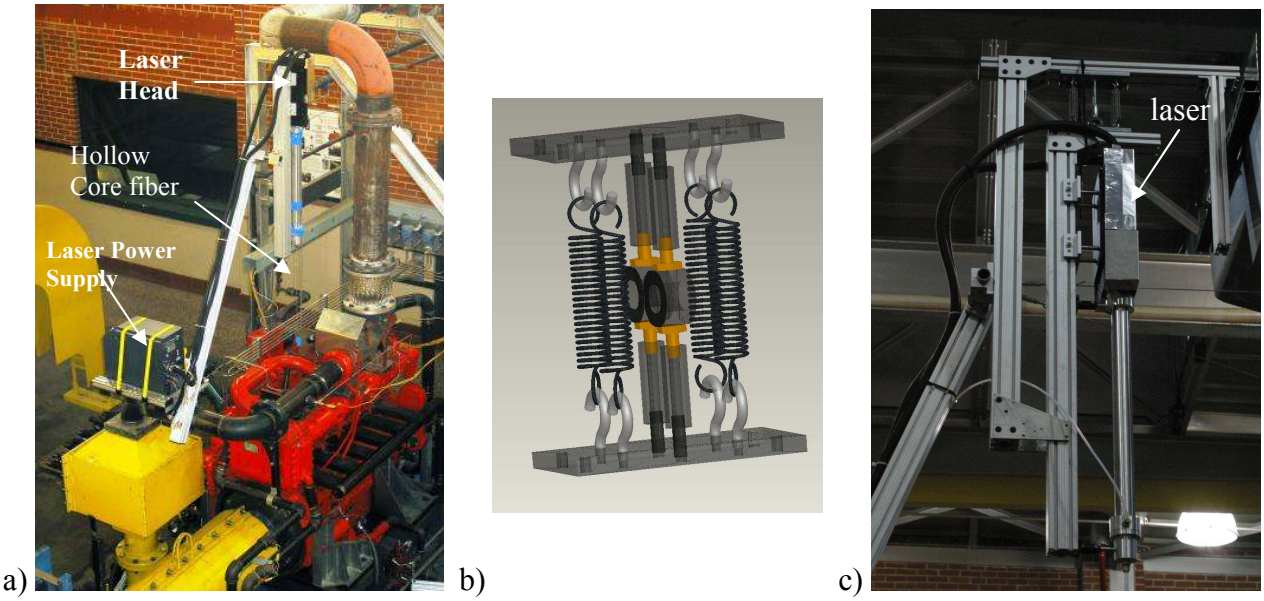

a) b) c)

Figure 18: Photos of the on-engine mounting assembly: a) view from above showing entire assembly, note laser power supply in lower left corner (exhaust head shield not shown); b) vibration damper used in the vibration isolation unit; c) mounting of the laser with the vibration damper and with the necessary frames to hold the laser ignition system above the engine.

4.2 Engine Controller

Figure 19 illustrates the equipment used to control the ignition timing and data acquisition. An oscilloscope provides real-time confirmation of ignition and verifies triggering alignment with TDC (top dead center). A high-speed data acquisition system (Hi-Techniques) records pressure data from the cylinder and sends a trigger to the pulse generator which is nominally 20-40 degrees BTDC (before top dead center). The pulse generator sends an output signal to trigger the laser firing (and thus the spark formation and cylinder ignition) by adding an appropriate delay to achieve the desired ignition timing.

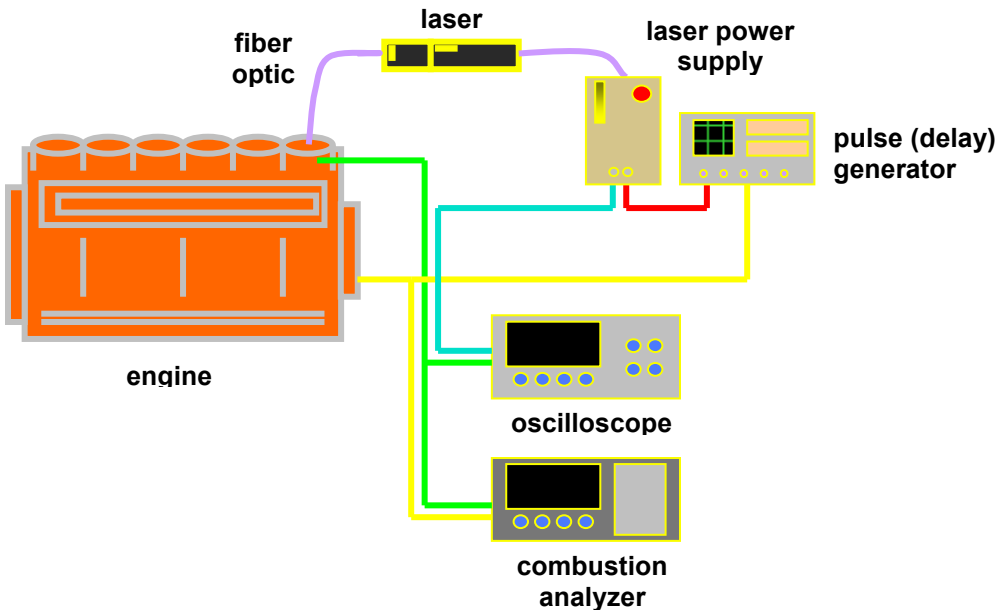

Figure 19 : A schematic of the timing control and data acquisition system

4.3 Engine Test-Results

The goal of these initial engine tests was to demonstrate successful fiber delivery, spark formation, and ignition. We used a single cylinder of an inline 6-cylinder Waukesha VGF turbocharged natural-gas engine to test the laser ignition system. The engine has a nominal rating of 400 bhp continuous at 1800 rpm. The engine displacement is 18 liters, with a cylinder bore of 5.98 inches and a stroke of 6.5 inches. Engine loading was achieved using a 1,200 hp Midwest eddy current dynamometer. For functional testing the engine speed was limited to 1500 rpm and load was limited to 35% of rated load. Lower loads are more challenging for laser ignition because of lower pressure and high-energy input for sparking and consequent ignition. It should be noted that higher loads are more favorable to optical spark formation due to higher initial pressure.

We attached the laser ignition system to cylinder number five, and the remaining cylinders (# 1-4, 6) were not altered and ran with conventional spark ignition. The timing of those cylinders was kept at the original setting, nominally 14° BTDC. However, the timing of the laser-ignited cylinder (#5) was controlled independently, and retarded to 8° BTDC. We didn't focus on the optimization of the engine but rather just focused on demonstrating a successful operation of a single cylinder using fiber delivery. The left of Fig. 20 shows the pressure traces of all cylinders, where each trace is an average of 1000 cycles. It was observed that even with the timing delayed on the laser-ignited cylinder, peak pressure was reached before all other cylinders, indicating an increased rate of heat release. The right of Fig. 20 shows peak pressure for 1000 consecutive combustion events in the laser-ignited cylinder. **During the engine operation, zero misfires were detected, demonstrating 100% reliability in the spark creation and combustion initiation. Thus, the tests succeeded in meeting the objective of demonstrating reliable laser spark delivery and ignition.** We note that this was the first demonstration of fiber delivered

spark ignition by any research group. In the right of Figure 20a periodicity can be observed with a period of approximately 75 cycles owing to problems with the governor.

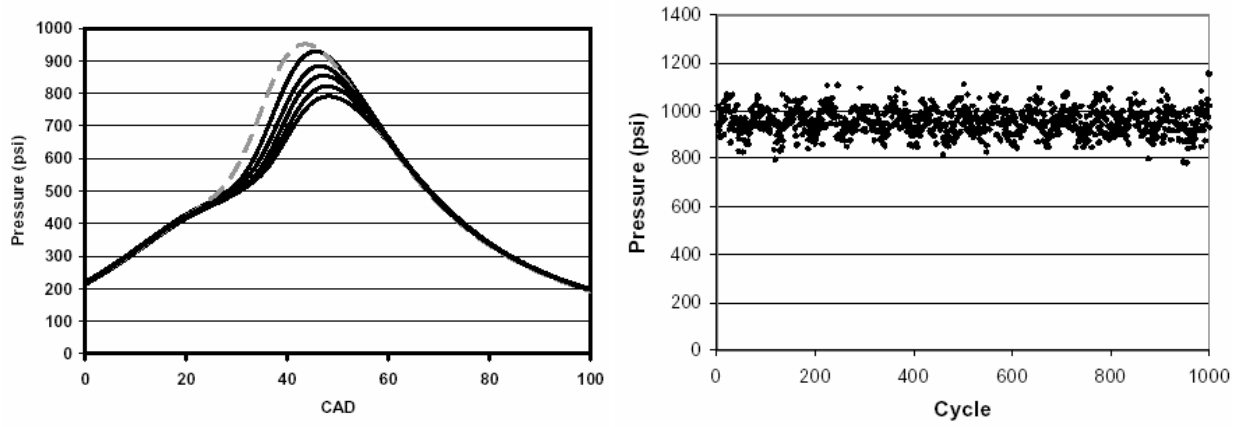

Figure 20: Left: Pressure curves for laser and electrical spark ignition. Laser ignition is used on cylinder #5 only (indicated by dotted curve). Right: Peak pressure data for the laser ignited cylinder (#5).

We have calculated the mass fraction burned as a function of crank angle for all cylinders using an averaged polytropic coefficient (determined by the Hi-Techniques combustion analyzer). The results are displayed in Figure 21 and Table 9. The results show that the laser ignited cylinder reached 10% mass fraction burned several degrees before any other cylinder, even though ignition timing was retarded by six degrees relative to the other cylinders. The burn duration from 10% to 90% is similar for all cylinders, which was anticipated, as the primary influence of laser ignition is an increased rate of flame kernel growth early in combustion. Once the flame kernel is established, the flame propagation rates through the cylinder should be similar. The data obtained during this round of engine testing supports this assumption.

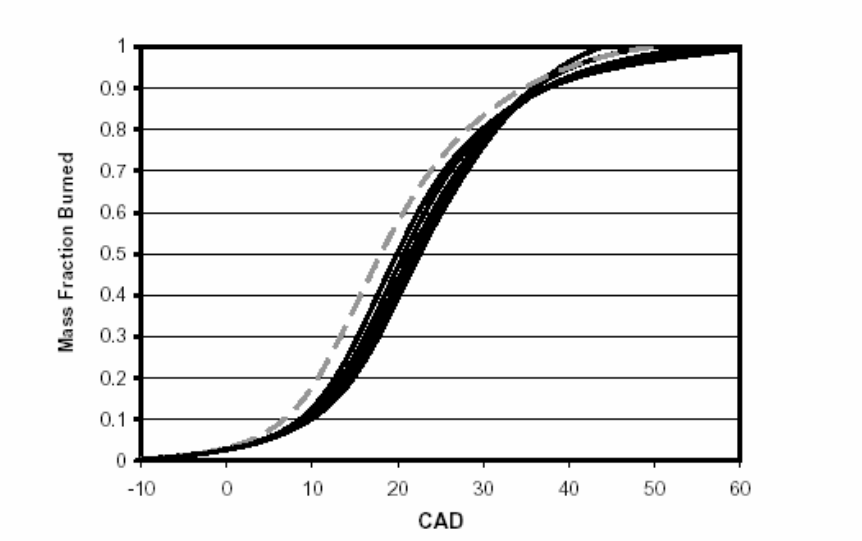

Figure 21: Mass fraction burned as a function of crank angle. Laser ignition is used on cylinder #5 (dotted curve).

Table 9: Burn durations, average peak pressure, and COV of peak pressure. Laser ignition on cylinder #5.

Cylinder #	*Spark Timing (°BTDC)*	*0-10% Burn (CAD)*	*10-50% Burn (CAD)*	*10-90% Burn (CAD)*	*Average Peak Pressure (psi)*	*COV of Peak Pressure (%)*
1	14	22.8	11.5	29.0	935	5.26
2	14	24	12.3	26.3	827	6.84
3	14	23.8	12.0	27.8	861	7.36
4	14	24	12.8	26.3	796	7.27
5*	8	15	11.8	28.0	957	5.65
6	14	23.3	11.8	28.3	890	6.05

5. Dual-Cylinder Testing on Caterpillar 3516C engine

We have conducted demonstrative two cylinder laser ignition on a 4-stroke Caterpillar G3516C series natural gas engine with 16 cylinders and speed of 1800 rpm. The engine has two banks with 8 cylinders on each side, as shown schematically in Figure 22.

5.1 Mounting Hardware

The selection of the two cylinders for testing was based on the following criteria:

1. Each cylinder needs to be sparked at 15Hz. The maximum firing speed of the laser is 30 Hz and is capable of sparking two cylinders. However, the cylinder timings must be opposite in the engine cycle in order to allow our laser to ignite both cylinders.
2. Second, the performance of end cylinders is characteristically different from the middle cylinders in the engine due to various factors such as mixing, poor fuel/air mixture distribution, jacket water cooling etc. Hence, we need two cylinders on the inside of the bank.
3. Third, maximum throughput for the fiber optics is achieved for a relatively straight fiber orientation, and currently, the maximum fiber length we can obtain for the hollow fiber is 2m. Therefore, the cylinders must be close together, in-line, and have no obstruction in the fiber path.

Given these constraints, cylinders 8 and 10 on the engine were chosen (see Figure 22). This will allow mounting of the laser and multiplexer in a horizontal orientation for use with our right-angle optical spark plugs and will require a minimum amount of curvature be imposed on the fibers. The optical spark plugs are as described in Section 3.2 and are shown below in Figure 23.

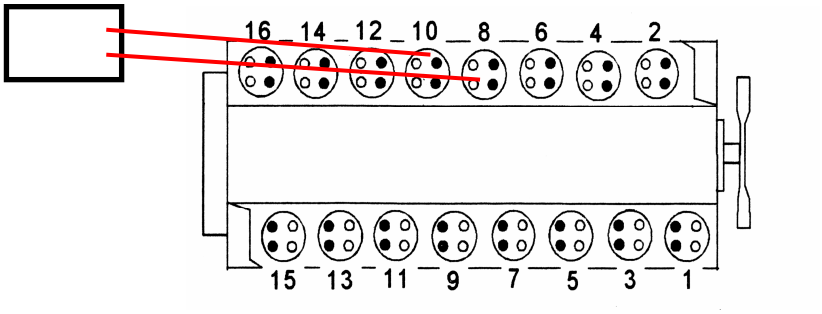

Figure 22: Diagram showing the engine from the top with the cylinders numbered. The box on the right shows the placement of the laser/multiplexer assembly, with the red lines showing the fibers going to their respective cylinders (in practice, the fibers will have some slight curvature).

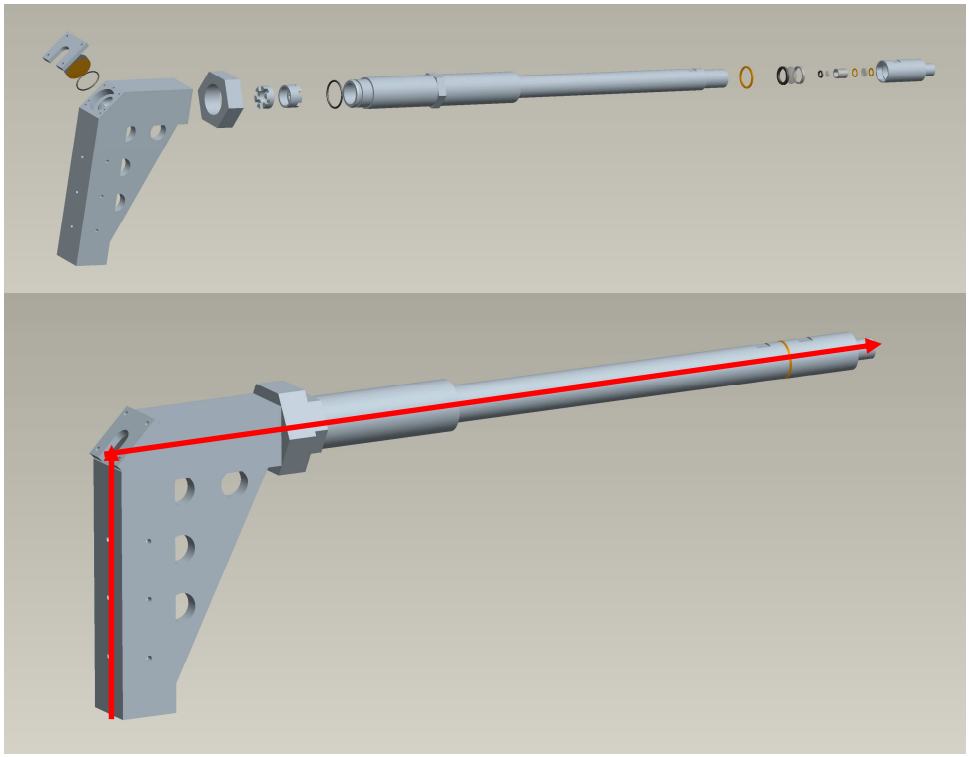

Figure 23: The optical spark plug exploded (top) and assembled (bottom). Shown in a horizontal position, the plug will in reality be vertical, with the right-hand barrel screwing in to the spark plug port on the cylinder. The fiber optic enters the plug on the bottom-right, and the beam is turned by a mirror at the top-right, where it then enters the barrel of the spark plug and the focusing optics (shown by the red arrows)

Figure 24 shows the system mounted on the engine. A reinforced base with supporting aluminum 80/20 was used to secure the multiplexer, mounted to the Woodward Control Panel. The whole multiplexer system (including the laser) assembly must be isolated from the engine vibration. This is achieved by isolating the rigid aluminum base-plate from engine vibration by a set of 4 air springs that can inflated to a design height to work within an optimum region. These air springs provide a low enough spring constant in the limited space under the multiplexer assembly that the resonant frequency is much lower than the engine vibration frequency (30Hz) and its first half frequency (15Hz), thereby providing adequate vibration isolation. A set of 4 rubber dampers are also installed to provide some level of damping. The assembly is placed in

line with the first bank of 8 cylinders (in which the two cylinders reside as chosen above), with the fibers exiting the multiplexer parallel to the floor, and going to each of the two cylinders on the engine.

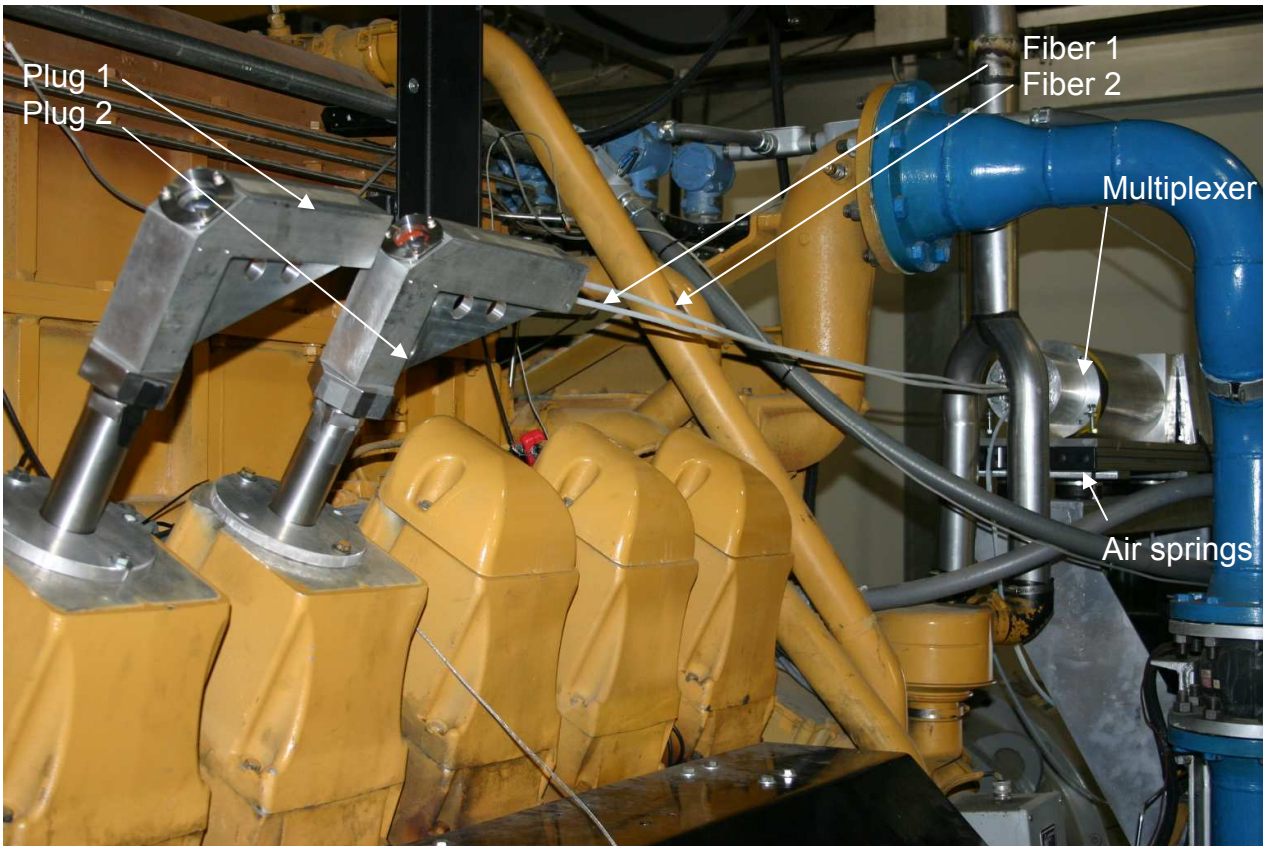

Figure 24: Engine mounting. Multiplexer with reinforced base sits on a set of six air springs on top of the C channel base plate mounted on the Woodward control box support. The two fibers extend from the multiplexer to the two spark plugs mounted on the cylinder 8 and cylinder 10 on CAT G3516C engine.

5.2 Engine Controller

The laser and galvanometer in the multiplexer are both controlled by a computer running a custom LabView program. The control system was modified in order to ensure proper synchronization with the engine. The LabView program controls a DAQ board which sets out a voltage from -10 to 10V to the galvo, thereby controlling the angular position of the steering mirror. In order to synchronize the galvo signals with the engine, two digital triggers are taken from a TTL pulse delay generator. The pulse generator itself is triggered from analog voltage signals from the inductive sensors attached to the ignition coil wires of the cylinders which fire immediately prior to the laser ignited cylinders. Because of the inability of the current DAQ card to handle both the high frequency galvo and the laser trigger signals from the same program, the two tasks are separated.

In order to fire the laser, another TTL pulse from the pulse delay generator is used. Once the steady state speed is reached, the delay time between the input analog trigger pulse and the laser firing pulse is set manually in the pulse delay generator and can easily be manipulated to advance or retard the spark timing.

In order to ensure the synchronization between the galvo position trigger and the firing laser trigger, an oscilloscope is used so that the appropriate galvo position (positive or negative voltage) coincides with the correct firing trigger (corresponding to the firing cylinder). For example, the firing trigger for cylinder number 8 needs to be associated with a negative voltage and vice-versa for cylinder number 10. This control system is designed just for the proof-of-concept. In practice, we envisage use of an FPGA programmed DAQ card for all hardware control.

5.3 Preliminary Engine Testing

Here results of preliminary dual-cylinder laser ignition tests are described. The tests were preformed on a 4-stroke Caterpillar 3516C series natural gas engine with 16 cylinders and speed of 1800 rpm. As discussed above, the spark plugs were mounted on cylinders 8 and 10 (see Fig. 22 and 24).

Initially, a number of dry runs were conducted in order to ensure proper synchronization of the multiplexer control system with the engine. Following the dry runs, fueled tests were conducted with fuel but at idle condition (1100 rpm). Two cylinders (numbers 8 and 10) were operated with laser ignition while the remaining cylinders operated with conventional ignition. It was observed that one of the two laser ignition cylinders (number 10) was igniting successfully, while combustion in the second laser ignition cylinder (number 8) was intermittent. The intermittency was attributed to misalignment in the fiber launch and/or the spark plug. (The two channels are in principle identical, so if one can spark reliably, then the other one should also.) Figure 25 shows images obtained at the optical access port of one of the spark plugs. (Light is captured through the 45 degree turning mirror which allows images from within the cylinder volume.) The left image shows light from the laser ignition spark while the right image shows combustion light (due to a successful ignition event). In the future, more sophisticated optical diagnostics will be conducted through this port.

Figure 25: Images obtained from laser ignited cylinder. Left: Laser initiated spark. Right: Subsequent combustion light.

These tests are viewed as successful proof of principle of the multi-cylinder laser ignition system. The following capabilities were demonstrated: mounting of system to engine, use of multiplexer to switch laser source to multiple cylinders, use of fibers to transmit laser pulses from source to cylinder, use of laser plugs to focus fiber delivered pulses to form sparks in cylinder volume, successful spark initiation and resulting combustion

6. Conclusions

Past research has shown that laser ignition provides a potential means to reduce emissions and improve efficiency of advanced high bmep gas-fired engines to meet longer-term DOE ARES targets. Despite the potential advantages of laser ignition, this technology has not been pursued commercially. A major impediment in this regard has been the "open-path" beam delivery in which the laser is delivered to engine cylinders from the laser source via a series of turning optics placed in the open air on, or near, the engine. This approach is not considered industrially practical owing to safety factors, as well as susceptibility to vibrations, thermal effects, etc. The overall goal of this project has been to develop and test practical laser ignition systems based on multiplexed fiber optic delivery. This report has summarized our progress in this regard. We have presented a theoretical (figure of merit) approach that has guided fiber selection and identified the potential use of hollow-core fibers. We have demonstrated sparking through coated hollow core fibers and their use for single-cylinder engine operation. We have shown bench-top multiplexing and dual-cylinder engine operation via multiplexed fiber delivered laser ignition. Besides the hollow core fibers, we have demonstrated sparking with fiber lasers. To the best of our knowledge, each of these accomplishments was a first.

It is worthwhile to consider the approaches developed here in the larger context of fiber-delivery approaches developed by other researchers. Fiber delivery approaches can be roughly divided into two categories depending on whether fibers are used to deliver high-power ignition pulses, or pump pulses to laser gain elements at the combustion location(s). In terms of the former, as we have focused on, delivery of high-power ignition pulses is challenging but progress has been made with both solid core fibers and coated hollow fibers. In both cases, relatively large diameter multimode fibers are required to deliver the high power pulses without exceeding the fiber damage threshold. For commonly used nanosecond laser sources, solid core fibers have not been demonstrated for delivery of pulses allowing spark formation in atmospheric pressure gases; however, sparks have been formed at elevated pressures (~5-10+ bars) where the breakdown intensity is lower. Coated hollow core fibers have been used to deliver sparks in atmospheric and elevated pressures as well as for engine ignition. The primary difference between the two types of fibers is in the smaller exit angle (higher beam quality) of the hollow fibers. Both types of fibers can tolerate moderate bending (down to radius of curvatures of approximately 0.5-1 m); however, bending losses in both types of fibers currently place some limitation on design flexibility and use.

Progress towards systems based on fiber delivered pump light has been achieved by other research groups. A trajectory of increased pulse energies and parameters has been demonstrated including published energies of 6 mJ for nanosecond pulses [30] which is a level comparable to that required in some applications. In a sense, the motivation to select such an approach is based

on avoiding the need to fiber deliver the actual igniting pulses. Our progress towards solving the latter problem decreases the need for fiber delivered pump approaches.

Spark formation has also been demonstrated at the output of fiber lasers. Owing to the inherent fiber coupling they provide, as well as their high efficiency and recent cost and performance trajectories, fiber lasers may provide attractive sources for laser ignition experiments. To date, output energies have been limited to several millijoules but approaches to raise the energy are available. Our demonstrative results with fiber lasers are included as Appendix A. Similarly, photonic crystal fibers (and photonic bandgap fibers) are attractive owing to their single mode output, but efforts are required to raise the maximum transmissible energies to levels useful in laser ignition. Both fiber lasers and PCFs have attractive bending characteristics in comparison to solid and coated hollow core fibers.

Fiber optic delivery is a key requirement to enable laser ignition technology to transition from research to commercial use. Significant progress has been made in terms of developing and testing the optical technologies required for fiber delivered laser ignition. This research has been discussed here, though for commercial acceptance factors such as lifetime, reliability and cost will need further consideration. In addition to providing robust ignition sources, the systems may open the door to new diagnostic capabilities. The fiber optics and window to the combustion volume also provide a means to extract light from the combustion chamber for diagnostic analysis. As an example, fiber delivered laser induced breakdown spectroscopy (LIBS) for fuel to air measurement has recently been demonstrated [31].

References

1. Lee, J.H., and Knystautas, R., *Laser spark ignition of chemically reactive gases.* AIAA Journal, 1969. **7**(2).
2. Ronney, P.D., *Laser versus conventional ignition of flames.* Opt. Eng., 1994. **33**: p. 510-521.
3. Dale, J.D., P.R. Smy, and R.M. Clements, *Laser ignited internal combustion engine-an experimental study.* SAE, 1979(SAE Paper 780329): p. 1539-1548.
4. Spiglanin, T.A., et al., *Time-resolved imaging of flame kernels: laser spark ignition of H2/O2/Ar mixtures.* Combustion and Flame, 1995. **102**: p. 310-328.
5. Phuoc, T.X. and F.P.White, *Laser-Induced Spark Ignition of CH4/Air Mixtures.* Combustion and Flame, 1999. **119**: p. 203-216.
6. Kopecek, H.e.a., *Laser ignition of methane-air mixtures at high pressures.* Exptl. Therm. and Fluid Sci., 2003. **27**: p. 499-503.
7. Herdin, G., et al., *Laser ignition-a new concept to use and increase the potentials of gas engines*, in *ASME Internal Combustion Engine Division 2005 Fall Technical Conference*. 2005. p. 1-9.
8. Bradley, D. and et. al., *Fundamentals of high-energy spark ignition with lasers.* Combustion and Flame, 2004. **138**: p. 55-77.
9. Gaborel, G., et al. *Toward the development of laser ignition system for aircraft engines*. in *Proceedings of First INCA, Workshop*. 2005. Snecma.
10. Stakhiv, A., et al., *Laser ignition of engines via optical fibers?* Laser Phys., 2004. **14**: p. 738-747.
11. Phuoc, T.X., *Laser spark ignition: experimental determination of laser-induced breakdown thresholds of combustion gases.* Opt.Commun., 2000. **175**: p. 419-423.
12. Rosen, D.I. and G. Weyl, *Laser-induced breakdown in nitrogen and rare gases at 0.53 and 0.35 um.* Journal of Physics D: Applied Physics, 1987. **20**: p. 1264-276.
13. Turcu, I.C.E., M.C. Gower, and P. Huntington, *Measurement of KrF laser breakdown threshold in gases.* Opt. Commun., 1997. **134**: p. 66-68.
14. Matsuura, Y., et al., *Hollow-fiber delivery of high-power pulsed Nd:YAG laser light.* Opt. Lett., 1998. **23**: p. 1858-1860.
15. Yalin, A.P., et al., *Use of hollow-core fibers to deliver nanosecond Nd:YAG laser pulses to form sparks in gases.* Optics Letters, 2005. **30**(16): p. 2083-2085.
16. Michaille, L., et al. *Damage threshold and bending properties of photonic crystal and photonic bandgap optical fibers*. in *Proc. SPIE 5618*. 2004.
17. Cheng, M.Y., et al., *High-energy and high-peak-power nanosecond pulse generation with beam quality control in 200?m core highly multimode Yb-doped fiber amplifiers.* Opt. Lett., 2005. **30**: p. 358-360.
18. Joshi, S., A.P. Yalin, and A. Galvanauskas, *Use of hollow core fibers, fiber lasers, and photonic crystal fibers for spark delivery and laser ignition in gases.* Applied Optics, 2007. **46**(19): p. 4057-4064.
19. Sato, S., et al. *Hollow-waveguide-based transmission of Q-switched Nd:YAG laser beam for biological tissue ablation*. in *Part of the SPIE conference on Speciality Fiber Optics for Medical Applications*. 1999.

20. Sato, S., et al., *Vacuum cored hollow waveguide for transmission of high-energy, nanosecond Nd:YAG laser pulses and its application to biological tissue ablation.* Optics Letter, 2000: p. 49.
21. Davis, J.P., et al., *Laser-induced plasma formation in Xe, Ar, N2, and O2 at the first four Nd:YAG harmonics.* Applied Optics, 1991. **30**: p. 4358-4364.
22. Tambay, R. and R.K. Thereja, *Laser-induced breakdown studies of laboratory air at 0.266, 0.355, 0.532, and 1.06?m.* J. Appl. Phys., 1991. **70**: p. 2890-2892.
23. Nubling, R.K. and J.A. Harrington, *Launch conditions and mode coupling in hollow-glass waveguides.* opt. Eng., 1998. **37**: p. 2454-2458.
24. Yalin, A.P. and e. al., *Laser ignition of natural gas engines using fiber delivery*, in *ASME ICE Division 2005 Fall Technical Conference*. 2005: Ottawa.
25. Inberg, A., et al., *Theoretical model and experimental studies of infrared radiation propagation in hollow plastic and glass waveguides.* Opt. Eng., 2000. **39**: p. 1316-1320.
26. Sircar, A., R.K. Dwivedi, and R.K. Thereja, *Laser induced Breakdown of Ar, N_2, and O_2 gases using 1.064, 0.532, 0.35 and 0.266um radiation.* Applied Physics B, 1996. **63**: p. 623-627.
27. Richou, B., I.G. Schertz, and J. Richou, *Delivery of 10 - MW Nd: YAG laser pulses by large-core optical fibers: dependence of the laser-intensity profile on beam propagation.* Applied Optics, 1997. **36**(7): p. 1610 - 1614.
28. Setchell, R.E., *Laser-injection optics for high-intensity transmission in multimode fibers*. 2000, Sandia National Laboratories.
29. Hand, D.P., et al., *Fiber optic beam delivery system for high peak power laser PIV illumination.* Meas. Sci Technol., 1999. **10**: p. 239-245.
30. Kofler, H. et al., *An innovative solid-state laser for engine ignition*, Laser Physics Letters, 2007. **4**: p. 322-327.
31. Dumitrescu, C. et al., *Fiber-Optic Spark Delivery for Gas-Phase Laser Induced Breakdown Spectroscopy* 2008 accepted for publication in Applied Spectroscopy

Appendix A - Fiber Laser

We have identified the fiber laser as a potential means of using fiber optics to deliver a pulsed laser beam in a way that allows spark formation and ignition. Very briefly, the fiber laser output allows the required combination of high power and high beam quality (requirements to achieve high intensity and to form laser sparks) in addition to high pulse energy (required to ignite mixtures). We have teamed with the research group of Dr. Almantas Galvanauskas (University of Michigan) who is one of the world leaders in the development of fiber lasers.

Our CSU team has visited and discussed with the Michigan group the technical requirements for spark formation and ignition, including approaches for focusing the fiber laser output to high intensities. This collaboration has recently resulted in a demonstrative "proof of concept" experiment that employed a fiber laser to form sparks in gaseous medium. This was the first demonstration of this kind with a fiber laser, and may also impact other fields, such as Laser Induced Breakdown Spectroscopy. The fiber laser employed is a laser in which the gain medium is the Yb-doped fiber. A 1064nm seed laser is coupled into the core of the fiber along with a 980 nm laser into the cladding. A fiber laser system (similar to that used in our experiments) is shown in Figure A1.

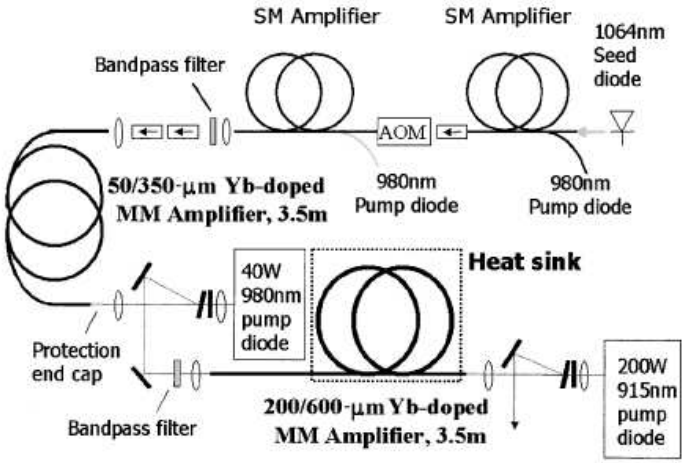

Figure A1. Fiber laser setup.

We have focused the output of the fiber laser system using low f# (short focal lens) optics to achieve small focal spots and high intensities. The experiment produced a laser spark in the room air as shown in Fig. A2, thereby showing the possibility of using the output of the fiber laser for spark formation. Experimental conditions were a pulse energy of several mJ and a pulse duration of ~1 ns. We are currently working on increasing the pulse energy so as to be better able to ignite lean mixtures, where pulse energies on the order of 10-20 mJ are typically required.

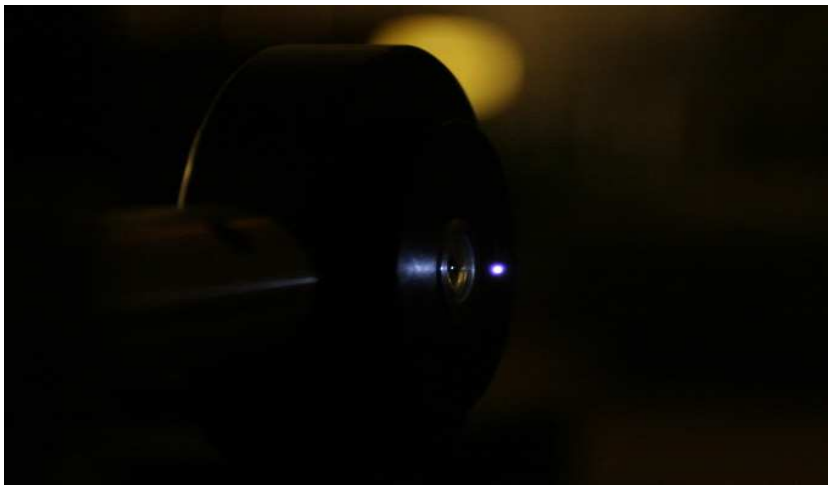

Figure A2. Spark Formation with fiber laser using 1064 nm light.

The above demonstration has shown the potential utility of the fiber laser as a means to fiber optically deliver sparks for practical laser ignition systems. The above demonstration employed a single spark from a single output, and we are currently discussing multiplexed approaches with the University of Michigan. The fiber laser used in the above experiments is a "one-off" scientific system and therefore relatively expensive. However, the cost trajectory for fiber lasers is very positive in the sense that the prices of the required components (primarily doped fibers and diode lasers) are rapidly decreasing**.**

Fiber lasers are a rapidly developing solid-state laser technology that holds high promise for practical laser ignition systems. In recent years the output parameters of pulsed fiber lasers have improved significantly, while costs continue to decrease. The main technological development that enabled this scaling is associated with fiber core size increase. Our recent work (in collaboration with the University of Michigan) has employed a multi-stage fiber amplifier system, seeded with electronically controlled nanosecond diode pulses, similar to the one described in [5]. As described in our past report we have experimentally verified that indeed laser-breakdown in air is achievable with nanosecond fiber laser pulses. Sparks were created in atmospheric pressure air by focusing 0.7-ns duration pulses from 80-μm core fiber amplifier (corresponding to 2.4-mJ pulse energy and 3.4-MW peak power) at 50-Hz repetition rate. This demonstration was the first proof that fiber lasers are well suited for formation of optical sparks.

Appendix B - Technology Transfer Activities

Refereed Journal Articles - Published

S. Joshi, A.P. Yalin, A. Galvanauskas, 2007, "On the Use of Hollow Core Fibers, Fiber Lasers, and Photonic Crystal Fibers for Spark Delivery and Laser Ignition in Gases" *Applied* 46, (19), pp. 4057-4064

A.P. Yalin, M. Defoort, B. Willson, Y. Matsuura, M. Miyagi, 2005, "Use of Hollow Core Fibers to Deliver Nano-second Nd:YAG Laser Pulses for Spark Formation*," Optics Letters* 30, pp. 2083-2085.

Refereed Journal Articles – In Press

A.P. Yalin, S. Joshi, M. DeFoort, B. Willson, 2007, "Towards Multiplexed Fiber Delivered Laser Ignition For Natural Gas Engines", accepted as Technical Brief in ASME Journal of Engineering for Gas Turbines and Power

Refereed Conference Proceedings/Transactions

S. Joshi, A.P. Yalin, C. Dumitrescu, S. Olcmen, P. Puzinauskas, 2008, "Laser Ignition and Laser Induced Breakdown Spectroscopy In Engines Using Hollow Core Fiber Delivery", accepted to Laser Applications to Chemical Security and Environmental Analysis (LACSEA 2008), Optical Society of America, St. Petersburg, FL

S. Joshi, A. Reynolds, B. Willson, A.P. Yalin, 2007, "Multiplexed Fiber Delivered Laser Ignition of Natural Gas Engines" ICE Division – ASME Fall Technical Conference, ICEF 2007-1617, Charleston, SC

A.P. Yalin, S. Joshi, A. Reynolds, M. Defoort, B. Willson, A. Galvanauskas, Y. Matsuura, M. Miyagi, 2006, "Fiber Delivered Systems for Laser Ignition of Natural Gas Engines" ICE Division – ASME 2006 Fall Technical Conference, ICEF 2006-1574, Sacramento, CA

A.P. Yalin, S. Joshi, M. DeFoort, B. Willson, A. Reynolds, Y. Matsuura, M. Miyagi, 2006, "Development of a Fiber Delivered Laser Ignition System for Natural Gas Engines", ICE Division – ASME Spring Technical Conference, ICEF 2006-1370, Aachen, Germany

A.P. Yalin, M.W. Defoort, S. Joshi, B. Willson, Y. Matsuura, M. Miyagi, 2005, "Laser Ignition of Natural Gas Engines using Fiber Delivery", ICE Division – ASME Fall Technical Conference, ICEF- 2005-2336, Ottawa, Canada

Refereed Conference Presentations, Posters, and Abstracts

A.P. Yalin, S. Joshi, A. Reynolds, B. Willson, A. Galvanauskas, 2006, "Fiber Delivered Systems for Laser Ignition of Nature Gas Engines", 3rd Annual Advanced Stationary Reciprocating Engines Conference, Argonne National Laboratory

Conference Papers and Presentations (Non-Refereed)

Defoort, A.P. Yalin, B. Willson, Y. Matsuura, M. Miyagi, 2005, "Hollow Core Fibers for Laser Spark Ignition in Natural Gas Engines", 2nd Annual Advanced Stationary Reciprocating Engines Conference, SCAQMD Headquarters, Diamond Bar, CA